<u>Reply to reviewers' comments on *"Core and margin in warm convective clouds. Part II: aerosol effects on core properties"*</u>

<u>Reply to reviewer #1</u>

General Comment

This paper follows from Part I which sought to examine the various methods of defining the cores and margins of convective clouds by using buoyancy, RH, and vertical velocity to define the core. They showed that these core diagnostics can be subsets of one another, but that this varies in space and time. This follow-on study examines the impacts of varying the aerosol concentration on the core definitions. Given that aerosols can change the cloud DSD, the condensation/evaporation rates can change, and thus the field RH, latent heating, and W. The authors effectively demonstrate the aerosol effects on the evolution of the convective cores and margins.

Main Comments:

Two main concerns that can readily be addressed are the need to:

MC1) Better state the goals and hypotheses of the study and state what makes this study novel compared to similar ones in the literature.

MA1) A paragraph was added to the introduction describing the novelty and goals of the paper: "***As a continuation to Part I of this work (hereafter PTI), in this part we analyze aerosols effects on the cloud's partition to core and margin throughout the lifetime of a cloud. We report the consequences these effects have on evolution of a cloud, in terms of volume, mass, and lifetime. As opposed to other works that typically focus on a single cloud core definition, here three different definitions are used (see Sect. 2), with emphasis put on the sensitivity of each core definition to aerosol concentration. Moreover, the combination of single cloud with large eddy simulations enables us to gain process level understanding and test the robustness of our findings.***".

MC2) Better reference past studies in the introduction relative to many of the scientific statements that are made regarding aerosol effects on cloud droplets.

MA2) We thank the reviewer for all the suggestions of additional references to this work, which were all implemented into the revised manuscript as described in the specific comments below.

Specific Comments:

SC1) Line 72-73: The warm phase convective invigoration process has brought about some lively debate in the community in recent years. It does seem however that lately more papers are being published on the matter. I would suggest adding a few additional references that may include the following:

Sheffield, A.M., S.M. Saleeby, and S.C. van den Heever, 2015: Aerosol-induced mechanisms for cumulus congestus growth. J. Geo. Res., 120, 8941-8952.

Saleeby, S.M., S.R. Herbener, S.C. van den Heever, and T.S. L'Ecuyer, 2015: Impacts of cloud droplet-nucleating aerosols on shallow tropical convection. J. Atmos. Sci., 72, 1369-1385.

SA1) We thank the reviewer for these additional references. They are now added to the text: "***The processes described above enable the more polluted cloud to condense more water and intensify its growth via increased release of latent heat (Kogan and Martin, 1994; Koren et al., 2014; Saleeby et al., 2015; Sheffield et al., 2015).".***

SC2) Lines 80-82: Perhaps add more recent references regarding impacts of aerosol and smaller cloud droplets on condensation and evaporation rates in clouds and along cloud edges.

Grant, L.D., and S.C. van den Heever, 2015: Cold pool and precipitation responses to aerosol loading: modulation by dry layers. J. Atmos. Sci., 72, 1398-1408.

Storer, R.L., and S.C. van den Heever, 2013: Microphysical processes evident in aerosol forcing of tropical deep convective clouds. J. Atmos. Sci.,70,430-446.

Saleeby, S.M., S.R. Herbener, S.C. van den Heever, and T.S. L'Ecuyer, 2015: Impacts of cloud droplet-nucleating aerosols on shallow tropical convection. J. Atmos. Sci., 72, 1369-1385.

SA2) Again, we thank the reviewer for bringing these references to our attention. We added them to the revised text: "***An opposite effect should take place in the sub saturated regions of the cloud, where more numerous and smaller droplets increase***

the evaporation rate and loss of cloud mass (Grant and van den Heever, 2015; Saleeby et al., 2015; Storer and van den Heever, 2013)."

SC3) Lines 86-88: This would be a good place to address the concept of "microphysical buffering". This has become much more prominent of a concept in the past few years.
SA3) The concept of microphysical buffering was added to the text, as follows: "***A different approach to aerosol effects suggests that cloud systems are buffered to microphysical effects (Stevens and Feingold, 2009). Several studies have shown that given enough time for the cloud system to reach steady state, cloud macro-physical parameters (e.g. cloud fraction, rain yield) show similar results for various aerosol concentrations (Carrió and Cotton, 2014; Glassmeier and Lohmann, 2018; Seifert et al., 2015).”***

SC4) Lines 97-99: Figure 17 of Khain et al. (2008, JAS) addresses this aerosol impact on various cloud types and cloud systems. This should be referenced.

SA4) Thank you for this suggestion, the reference was added to the relevant line.

SC5) Lines 100-110: This paragraph should cite Reutter et al. (2009) with respect to the "aerosol-limited" vs "updraft-limited" regimes. Looks like you already have this paper in your reference list, but it would be good to add the citation in this paragraph.

SA5) Agreed, the reference was added to the relevant paragraph as follows: "***Based on the idea that clouds can be partitioned to aerosol-limited, updraft-limited, or aerosol and updraft sensitive regimes (Reutter et al., 2009), a unified theory for the contradicting results regarding aerosol effects was suggested (Dagan et al., 2015)”.***

SC6) Line 140: Here you are transitioning from the paper introduction to the methods section. Your introduction is very thorough, but you haven't yet stated the goals or science questions of the paper. Please make sure you tell your audience the purpose of the paper and why it is important and novel.

SA6) Thank you for this comment, we have added a paragraph explaining the goals of this paper (see MA1 above).

SC7) Lines 239-244: Things get a bit confusing when you refer to precipitation and evaporation of droplets. It's not clear if you're referring to "cloud droplets" or "rain drops". It would be helpful if cloud hydrometeors are always referred to as "droplets" and rain (precipitation) as "drops". So, are you indicating here that the clean case leads to larger cloud droplets and larger rain drops?

SA7) In these sentences we are referring to the entire distribution of drops, which is skewed to larger sizes in clean cases. For clarity, we switched the word droplet to the more general word drop: "***Moreover, the occurrence during precipitating stages and for lower aerosol concentrations indicates that slow evaporation due to larger drop sizes is crucial.***".

SC8) Lines 308-316: This is just a comment, but I appreciate your analysis here and how you allude to polluted clouds essentially mimicking a saturation adjustment with respect to condensation, and how clean clouds allow substantial supersaturation to be carried about. Given that saturation adjustment schemes are still often used in microphysics parameterizations, this re-emphasizes that use of such a scheme can be very inappropriate except under specific circumstances.

SA8) Thank you for the comment. We have seen such mimicking effects in previous work as well (Heiblum et al., 2016b).

SC9) Section 4: Moving into this section reminded me to ask about how your aerosols are treated in the model following initialization. Are the initial aerosol concentrations homogeneous in 3D, do the aerosols advect around the domain, are aerosols removed upon nucleation and regenerated upon droplet evaporation? Are there aerosol sources and sinks? This could certainly be of most importance in a field of clouds.

SA9) Thank you for this important comment. To answer your questions, aerosols are initialized homogeneously in 2D (horizontally), maintaining constant mixing ratio with height. They are advected around the domain, and are removed upon nucleation and regenerated upon evaporation. Wet scavenging serves as a sink, while there are no sources. We added some details about how the model treats aerosols and a relevant reference (Heiblum et al., 2016a) for a more complete description: "***To study the effects of aerosols on the cloud cores we run each model setup with three different aerosol concentrations: clean – 25 cm^{-3}, intermediate – 250 cm^{-3}, and polluted – 2000 cm^{-3}. The model domain is initialized using an oceanic size distribution (Altaratz et al., 2008; Jaenicke, 1988), maintaining constant mixing ratio with height. Aerosol budget includes removal by nucleation and regeneration upon evaporation, while wet scavenging by precipitation removes aerosols from the domain. Thus, the aerosol concentration may be depleted by 20%–40% (depending on the precipitation amount) during the simulation. More on the treatment of aerosols in the cloud field model can be found in previous work (Heiblum et al., 2016a)***.".

SC10) Figure 5: Why is the inversion layer base height higher in the clean case? I don't recall this being addressed in the paper. Is it initially the same in all cases and then changes over time due to microphysical and dynamical interactions?

SA10) As guessed correctly by the reviewer, the inversion base height is initially the same for all cases and evolves differently with time. We now address this point in the paper: "***It should be noted that horizontal dashed lines in Fig. 5 represent the inversion base height after 5 hours of simulation (approximately middle of simulation), where an increase in the inversion base height is seen with decrease in aerosol concentration. This is due to increased net warming in the upper cloudy layer (i.e., release of latent heat during condensation with reduced local evaporation) with increase in precipitation (Dagan et al., 2016; Heiblum et al., 2016b) , which raises the inversion base".***

SC11) Line 579: When you refer to evaporation throughout the paper are you referring to partial evaporation as a process or fully evaporated droplets? This could be clarified a bit in the paper. Many past papers including some cited herein often refer to net evaporation of drops/droplets as a distribution without specific concern for full evaporation of droplets.

SA11) Thank you for this comment that helped us clarify this point. Throughout the paper we refer to evaporation as a process (i.e. mass evaporated per second [g/s]), and hence many times mention evaporation rates rather than how many droplets were fully evaporated. We added a short sentence to the introduction to clarify this point:

“***Henceforth evaporation will be referred to as a process (i.e. change of mass per unit time) rather than complete evaporation of a water drop.”***

SC12) Summary section: I find the summary to be a bit over-comprehensive. It’s helpful to the reader to keep this concise and to the point. Keep to the main conclusions and main mechanisms. Details can be seen in the bulk of the paper.
SA12) After rereading the summary, we agree with this comment. The summary has been shortened considerably.

SC13) Figures: My main comment about the figures is that most of the them need to be larger, especially the fonts, so that they are easily readable.
SA13) All the figures were redone so that the fonts are larger and readable.

SC14) Line 302: Should read as “and enables it to live for…”
SA14) Thank you, the suggested correction was carried out.

SC15) Line 426: Should read as “segments which shed off the main…”
SA15) Thank you, the suggested correction was carried out.

SC16) Line 449-451: I find the wording here to make the sentence confusing. Please try clarifying this sentence.
SA16) The sentence was rephrased as follows: “***In contrary, pixels fractions of Bcore inside Wcore span the entire range of values (i.e. partial overlaps between the core types), as seen for both single clouds and cloud fields during dissipation***”

SC17) Line 521-522: This is a bit of a run-on sentence with a comma separator.
SA17) We have changed the sentence as follow: “***In Fig. 9 we check how these aerosol effects are manifested in the cloud field scale (using the CvM space) by observing the mean relative humidity (RH) in the cloud core and margin of all clouds, where the core (margin) mean RH can be taken as a proxy for condensation (evaporation) efficiency***”.

SC18) Line 656: This should read as “However, except for the…

SA18) Thank you, we have reformulated the sentence: "***However, excluding the initial time of cloud formation where the entire cloud is super-saturated, clean clouds tend to be margin dominated in terms of volume for most their lifetimes***".

Reply to reviewer #2

General Comment

In the study effects of aerosols on the structure of small CU are investigated by analyzing

the results of axisymmetric cloud model (single cloud simulations), as well as model of cloud ensemble (SAM) (for investigation of general properties of cloud ensembles). To shorten number of parameters, cloud averaged properties are analyzed. Clouds are characterized by core and margin, and effects of aerosols on these regions are investigated. The paper is of interest. However, major revision is necessary.

Main Comments:

MC1) Figures 5, 7, 9 indicate that simulation with low aerosol concentration was performed for inversion base at 2000 m, while in other simulations the inversion base was at 1500m. Since the cloud dynamical and microphysical structure as well as cloud size depend on the inversion height, the comparison of the aerosol effects should be performed under similar thermodynamic background conditions.

MA1) Thank you for this important comment that helped us clarify our method. All simulations were initialized using the same thermodynamic profile. Figs. 5, 7, 9 show the inversion base height after 5 hours of simulation (and not the initial state), and thus are not equal for different simulations because of microphysical and dynamical interactions between the clouds and their environment that modify the temperature profile of the domain. We choose to display this inversion height (rather than the initial one which is equal for all simulations) since it better reflects the CvM space cloud scatter of the entire simulation. We added to the revised version an explanation clarifying these differences: "***It should be noted that horizontal dashed lines in Fig. 5 represent the inversion base height after 5 hours of simulation (approximately middle of simulation), where an increase in the inversion base height is seen with decrease in aerosol concentration. This is due to increased net warming in the upper cloudy***

layer (i.e., release of latent heat during condensation with reduced local evaporation) with increase in precipitation (Heiblum et al., 2016b), which raises the inversion base".

MC2) The terminology used in the study is not widely accepted and needs better definition. For instance, it is necessary mathematically define what is "condensation efficiency", "diffusion efficiency", etc. (It is possible that such definitions are in Pt 1 of the study. Nevertheless, they should be defined in the present study as well). Note that in addition to equation of diffusion growth ("diffusion efficiency"), there is a turbulent diffusion.

MA2) We have reviewed the terminology used in the work and defined it when necessary. For the example of diffusion efficiency: "***We note that throughout this work the word* efficient *will be used to describe both the rate and the total change of mass attributed to a microphysical process.***". This definition is based on the multiple references and descriptions listed in the introduction section.

MC3) Different definitions of cloud cores and cloud margin are interesting. At the same time, these definitions do not agree with the accepted ones. Such definitions lead to a paradox that small dissipating clouds may contain cloud cores. Supposedly, some minimum LWC value should be included into the definition. This will exclude cases, when dissolving cloud with negligible LWC is still considered as combination of cloud core and cloud margin.

MA3) As reported in Part I, we do take a minimum threshold of 0.01 g/kg for definition of a cloudy pixel. As a matter of fact, we were questioned about the LWC threshold during the review process of Part I, and showed that this definition best captures the main cloudy processes of condensation and evaporation. We quote our answer here. "***The question of cloud pixel liquid water content (LWC) threshold is something we have examined as part of this work. We started by taking an even lower threshold of 0.005 g/kg (Cohen and Craig, 2006) but eventually raised the threshold to 0.01 g/kg based on other works (Jiang et al., 2009; Xue and Feingold, 2006). The impact of threshold choice is shown in Fig. RA1 below. The 0.01 and 0.005 g/kg thresholds yield similar results with regards to cloud volume, while higher thresholds (0.05 and 0.1 g/kg) reduce cloud volume significantly. By taking areas of condensation and evaporation as indicators of cloudy regions, it can be seen that the higher values thresholds "miss" pixels with high evaporation rate (vapor diffusion), in both***

growing and dissipating stages of cloud lifetime. Hence, we find that the 0.01 g/kg threshold best reflects a cloudy volume, without the risk of including insignificant cloud debris as can be seen in some cases for the lower 0.005 g/kg threshold.".

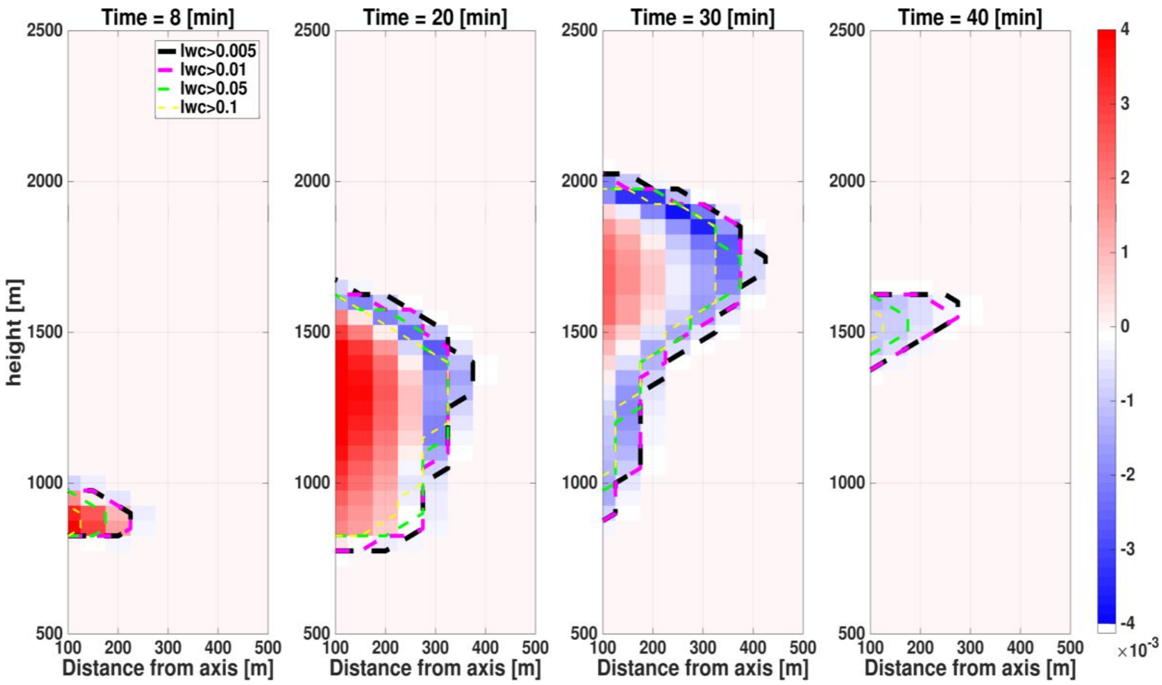

Fig. RA1. Four vertical cross-sections (at t=8, 20, 30, 40 minutes) during the single cloud simulation with aerosol concentration of 500 CCN. Y-axis represents height [m] and X-axis represents the distance from the axis [m]. The black, magenta, green and yellow dashed lines represent different LWC thresholds for a cloudy pixel (see legend for values). The background represents the condensation (red) and evaporation rate (blue) [g kg^{-1} s^{-1}].

Specific Comments:

SC1) line 24 Abstract. The values Bcore, Rcore, Wcore are not defined yet and should be either defined or excluded from the abstract.

SA1) A sentence defining the mentioned values was added to the abstract: "***Three core definitions are examined: positive vertical velocity (Wcore), supersaturation (RHcore), and positive buoyancy (Bcore).***".

SC2) Line 45. The text reads: “detrainment while losing mass”. In cloud physics detrainment is “large scale” outflow, typically near cloud top. Interaction of clouds with environment is characterized by entrainment and mixing. The authors supposedly mean that small cloud volumes leaving the parent cloud loss their mass by evaporation.

SA2) Based on our understanding detrainment is the same as entrainment, just opposite wind flow (see AMS glossary). A cloud cannot expand horizontally (which is the case here) by entrainment, only by detrainment where the wind vectors are from in the cloud outwards. After detrainment into the non-cloudy environment, mixing occurs and the final result is either a cloudy (with less LWC) or non-cloudy pixel. We try to clarify the sentence as follows: ***“In clean clouds larger droplets evaporate much slower, enabling preservation of cloud size and even increase by detrainment and dilution (volume increase while losing mass)***”.

SC3) Line 57. what difference of DSD do you mean?

SA3) The differences in DSD mentioned in line 57 are explained in the following line in the text. We have reformulated these few sentences in order to avoid confusion (see also SA4 below): “***Aerosols act as cloud condensation nuclei (CCN) during heterogeneous nucleation of cloud droplets(Köhler, 1936; Mason and Chien, 1962).The number, size, and composition of aerosol distribution yields differences in the initial cloud droplet size distribution (DSD). Polluted clouds (i.e. more aerosols) have more, but smaller droplets, and a narrower DSD compared to clean clouds (Andreae et al., 2004; Twomey, 1977).”***.

SC4) Line 58. The sentence is not clear or not correct. The nucleation itself that takes place at rN>rNcrit does not accompanied by decrease of S. S decreases as a result of diffusional growth of nucleated droplets.

SA4) Thank you for this comment. We did not intend to say supersaturation is reduced by nucleation, but rather the existence of aerosols enable droplet activation in lower S than in a pristine atmosphere with no aerosols. We have changed this part to be clearer, as seen in SA3 above.

SC5) Line 77. Strictly speaking, the diffusion growth equation is not symmetric with respect of processes of condensation/evaporation. This asymmetry is considered, sometimes, as a mechanism of DSD broadening (e.g. Korolev, 1995, JAS, 52, 3620-3634).

SA5) Thank you for this comment. Analytically speaking, the diffusion equation should be symmetric for condensation and evaporation, but this is only in theory. Thus, we have removed this sentence from the revised text.

SC6) Line 161. Comment concerning the cloud core definitions. The condition W>0 takes place in cloud cores of devolving clouds. Since the time period of cloud developing is relatively short, effects of mixing with surrounding air may not be significant (depending of cloud size and W). At dissolving stage, W<0. So, there is no cloud core in your definition. At the same time LWC in the cloud may has obvious maximum in the cloud center (interior).

SA6) We note that our choices of cloud core definitions are based on previous works, as listed in Part I: "***Considering convective clouds, there are several objective measures that have been used in previous works for separating a cloud's core from its margins (will be referred to as physical cores hereafter). In deep convective cloud simulations the core is usually defined by the updrafts' magnitude using a certain threshold, usually W>1 m·s^{-1} (Khairoutdinov et al., 2009; Kumar et al., 2015; Lebo and Seinfeld, 2011; Morrison, 2012). Studies on warm cumulus clouds have defined the clouds' core as parts with positive buoyancy and positive updrafts (Dawe and Austin, 2012; de Roode et al., 2012; Heus and Jonker, 2008; Siebesma and Cuijpers, 1995) or solely regions with positively buoyancy (Heus and Seifert, 2013; Seigel, 2014). More recently, cloud partition to regions of supersaturation and sub-saturation has been used to define the cloud core in single cloud simulations (Dagan et al., 2015).***".

To our knowledge, previous works use a LWC threshold for cloud definition but never for core definition. The case the reviewer describes where LWC has a maximum in the cloud center (or RHcore for example) and there's no Wcore may indeed exist. Due to that, in Part I we define a cloud geometrical core (center of gravity or centroid), and compare its location with the cloud physical core (Wcore, RHcore, Bcore). We quote some of the conclusions here: "***With respect to cloud morphology, the majority of clouds are composed from single cores (for all core types), located near the cloud centroid/COG, and fit the intuitive core-shell model of decreasing core parameter values from cloud center to periphery. This is especially true during cloud growth, as***

during dissipation the cores may decouple from the geometrical core and often comprise just a few isolated pixels at the cloud's edges. ".

Regarding the Wcore definition, we quote from Sect 2.3 in Part I: "***We note that setting the core thresholds to positive values (>0) may increase the amount of non-convective pixels which are classified as part of a physical core, especially for the Wcore. Indeed, taking higher thresholds for the Wcore (e.g. $W > 0.2\ ms^{-1}$) decreases the Wcore extent in the cloud and reduces the variance of Wcore fractions between different clouds in a cloud field (as seen in Fig. 4). Nevertheless, any threshold taken is subjective in nature, while the positive vertical velocity definition is process based and objective.***".

Later in that paper, we show that the Wcore is actually much more "well-behaved" than expected, so that clouds typically have a single Wcore, rather that multiple small Wcores around the cloud. As is written in the text: "***For the Bcore, RHcore, and Wcore, 68%, 79%, and 81% of the cloud scatter analyzed (which contain a core) have a single core, respectively. Thus, most clouds have a single core. Moreover, it is more probable to find multiple buoyancy cores in a cloud than vertical velocity cores. This is surprising given our choice of "weak" Wcore thresholds (i.e. positive values) and indicates that vertical velocity patterns are relatively well-behaved in cumulus clouds, at least for the LES scales chosen here.***"**.**

SC7) line 184. How can be explained updrafts at B<0? Gravity waves?

SA7) Similar to answer SA6, this issue is also treated in details in Part I. Specifically, updrafts with negative buoyancy are a very common feature in shallow cumulus fields. This issue is discussed in depth in Part I, here we quote some of the relevant text: "***…for the adiabatic column case, Bcore is always a proper subset of Wcore (i.e. Bcore ⊂ Wcore. These effects are commonly seen in warm convective cloud fields where permanent vertical layers of negative buoyancy (but with updrafts) within clouds typically exist at the bottom and top regions of the cloudy layer (Betts, 1973; de Roode and Bretherton, 2003; Garstang and Betts, 1974; Grant and Lock, 2004; Heus et al., 2009; Neggers et al., 2007).***", and also: "***The vertical velocity equation dictates that buoyancy is the main production term (de Roode et al., 2012; Romps and Charn, 2015), and is balanced by perturbation pressure gradients and mixing (on grid and sub-grid scales). Thus, all changes of magnitude (and sign) in vertical velocity should***

lag the changes in buoyancy. This is the basis of convective overshooting and cumulus formation in the transition layer".

SC8) Line 200. In such case it is difficult to call the condition W>0 as definition of cloud core. Small positive W can take place all over cloud just by turbulent fluctuations. Katzwinkel et al. (2014) and Schmeissner et al. 2015 determine cloud interior as LWC>0.2 gm^{-3} this condition guaranties that the region chosen is in the cloud interior.
SA8) We note that the purpose of these papers (including Part I) is to gain the most general understanding on the partition of cloud to core and margin, using the most general definitions. As mentioned in MA3, applying a LWC>0.2 gm^{-3} threshold can exclude much of the cloud, while our goal is to look at the entire cloud. Regarding small W, as explained in SA6 above, adding random thresholds for a core definition is unphysical in our opinion, and can be very sensitive to a specific model or case study. On the other hand, taking positive vs. negative values partitions the cloud based on purely physical considerations, that can also be applied to other works. Nevertheless, as shown in SA6, the occurrence of small positive W pixels is less common than one would think. Thus, for sake of consistency and generality, once a definition is set for cloud core, even a small Wcore like the one mentioned in line 200 is considered a core.

.

SC9) line 202. Fig 1. Figure caption. Define LHS axis, RHS axis. What is "other core types"?
SA9) Thank you, we have changed LHS and RHS to left axis and right axis. The caption was rephrased as follows: "***Time series of pixel fractions [%] of one core type within another, for the respective simulation types***".

SC10) lines 236-240 The mechanism proposed requires additional justification. The other option is that in low CCN case drizzle and rain drops rapidly fall down, so LWC is very low in the subsiding of the air. Another possible mechanism is turbulent mixing between warm core and colder margin air. This mixing should lead to an increase in T, i.e to appearance of positive buoyancy. Can you justify the mechanism that is proposed in the study? What is the cloud stage? Developing or dissolving? Do you see this effect at cloud center or cloud periphery?
SA10) The mechanism we suggest for the pockets of positive buoyancy has been thoroughly checked and is a major part of this paper. We start Sect. 3.2 by noting a

main point from Part I, that mixing of cloudy and non-cloudy air or core with margin air almost always (except extreme unlikely cases) reduces buoyancy: "***The theoretical arguments in PTI showed that B_{core} should be the smallest of the three. This was shown for both the adiabatic cloud column case and also the non-adiabatic case where entrainment mixing and consequent evaporation has a strong net negative effect has on cloud buoyancy***". The other option that the reviewer is referring to is the depletion of LWC and hence a smaller water loading term in the buoyancy equation, however, this was checked and the water loading term is as large in the positive buoyancy pockets as in their surroundings. We added this sentence to the text: "***The liquid water content buoyancy term (not shown here) is always negative and typically increases (in absolute value) with increase in vertical velocity or total buoyancy***".

Throughout the paper (see Figs. 5, 7) and also in Part I (see Fig. RA2 below), we find these pockets of positive buoyancy mostly during late mature and dissipation stages of the cloud, after the initial main convective core has disappeared. This effect is mostly attributed to the cloud periphery but can also be in the cloud center for small dissipating clouds. Both sections 3.2 (for single cloud) and 4.2 (for cloud field) provide proof and attempt to justify the assumption that positive buoyancy is formed due to heating in downdrafts during cloud dissipation.

Finally, we have altered the definition of this effect from "adiabatic heating" to "downdraft buoyancy production" and added a more rigorous description of the effect based on previous theoretical and observational works. The description is as follows: "***Although not usually the focus of studies, the existence of positively buoyant downdrafts in convective clouds has been reported in both observations (Igau et al., 1999; Wei et al., 1998) and simulations (Xu and Randall, 2001; Zhao and Austin, 2005a, 2005b). A possible explanation for this can be deduced from previous theoretical studies predicting mixing induced downdrafts in cumulus clouds (Betts and Silva Dias, 1979; Betts, 1982). It was shown that in some cases cloud - environment mixtures are negatively buoyant (while still containing liquid water) and the consequent downdrafts can sometimes descend only part way down to the cloud base before reaching neutral buoyancy. Similar to convective overshooting, parcels with negative vertical momentum may then "undershoot" the downdraft equilibrium level and turn positively buoyant while the downdraft weakens. One can therefore expect the magnitude of positive buoyancy within the downdraft to reach a maximum when the***

velocity approached zero. Hereafter we refer to positive buoyancy production within downdrafts as downdraft buoyancy.

Downdraft buoyancy production occurs frequently in cumulus fields because the negatively buoyant downdrafts follow a warming lapse rate which is more unstable than the environmental one, which is typically between the dry adiabat and moist adiabat (as is the case for the Hawaiian and BOMEX profiles simulated in this work). On one extreme, a descending parcel is least buoyant (i.e. coolest) when evaporation (after mixing) keeps it just barely saturated (Paluch and Breed, 1984)(also PT1) so that the lapse rate of descent tends to moist adiabatic and may remain negatively buoyant. On the other extreme, if little to no evaporation of liquid water occurs, the descent will follow the dry adiabat and switch to neutral (and then positive) buoyancy rapidly. Thus, the ability of a negatively buoyant cloudy downdraft to sustain itself depends on continuous inflow of liquid water (by mixing) and its consequent evaporation (Knupp and Cotton, 1985). “.

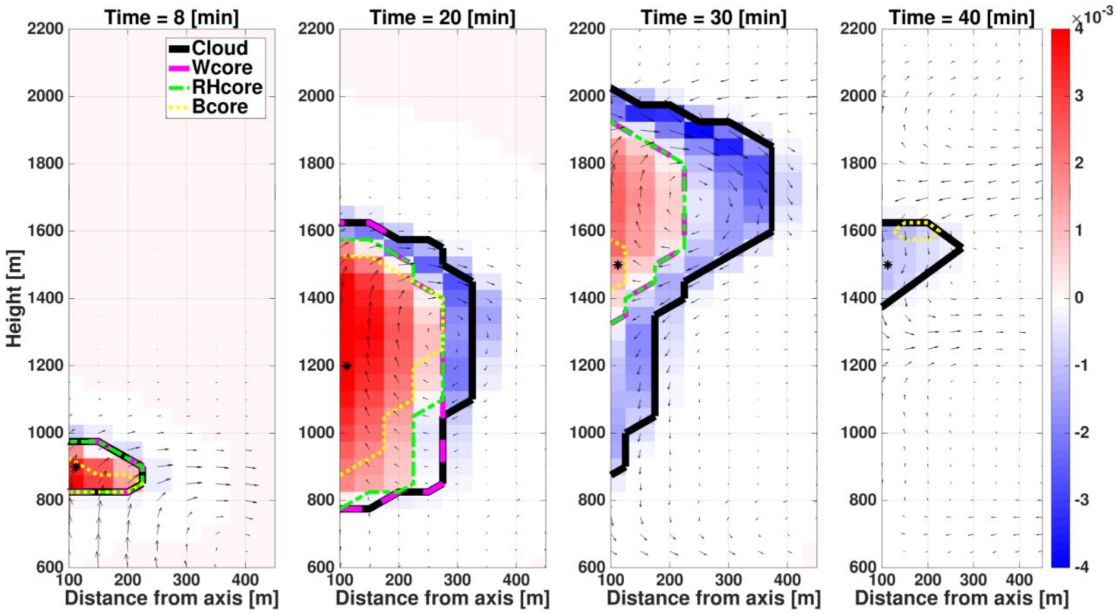

Figure RA2. Four vertical cross-sections (at t=8, 20, 30, 40 minutes) during the single cloud simulation. Y-axis represents height [m] and X-axis represents the distance from the axis [m]. The black, magenta, green and yellow lines represent the cloud, W_{core}, RH_{core} and B_{core}, respectively. The black arrows represent the wind, the background represents the condensation (red) and evaporation rate (blue) [g kg^{-1} s^{-1}], and the black asterisks indicate the vertical location of the cloud centroid. Note that in *some cases the lines indicating core boundaries overlap (mainly seen for RH and W cores).*

SC11) Line 248 How is cloud margin region defined and calculated?

SA11) Core and margin are defined according to the three definitions used throughout the paper, Wcore, Bcore, and RHcore. We reformulated the sentence to clarify this point: "***Here we evaluate how aerosol effects within the core and margin (using the three core definitions) affect the cloud characteristics***".

SC12) line 254. It is difficult to see the non-monotonic dependence. We see that the maximum cloud mass takes place at high CCN concentration, but lifetime is larger for the low CCN concentration case.

SA12) The non-monotonic dependence referred to in that specific sentence is only that of total cloud mass, as quoted from the text: "***A non-monotonic dependency of total cloud mass on aerosol concentration is seen, showing a maximum for the intermediate concentration. This type of dependency has been previously reported for warm cumulus clouds (Dagan et al., 2015; Savane et al., 2015).***". The effect isn't very large, but in Fig. 3 it is clearly seen that the intermediate concentration reaches the maximum total mass. References for this behavior are given.

SC13) line 285. I do not fully agree with the interpretation. In case of high CCN concentration droplets are small and mixing with surrounding leads to fast complete evaporation of the droplets. Moreover, small droplets fully and easily evaporate also at W<0. At the same time, larger droplets formed at low CCN concentration evaporate only partially. Why is it necessary to focus on the weak effect of the differences in the evaporation rates?

SA13) Thank you for this comment. We agree with the reviewer that there are additional parts in the interpretation that should be explained in more details beside the part of differences in diffusion efficiencies (which includes different rates and different droplet surface areas for diffusion process to occur). We now also emphasize the different DSD before evaporation starts which impact the cloud lifetime and cloud volume. Here are a few changes in the text: "***These results with respect to cloud volume***

can be attributed to the smaller drop sizes and higher diffusion efficiencies with increase in aerosol concentration.", and: "***The polluted cloud is composed of small drops, evaporates its margin regions efficiently, and is thus limited in dilution growth. The clean cloud is composed of larger drops, less efficient in evaporating its margins, and hence can grow by dilution of its LWC upon a larger volume.***", and: "***The clean cloud shows opposite behavior, with extremes of large super-saturation during cloud growth (initial stages) and large sub-saturation during cloud dissipation (final stages). The large super-saturation can be explained by the low diffusion efficiency, but the large sub-saturation also takes into consideration the larger drop sizes which take more time to evaporate***"

SC14) line 293 At the dissolving stage cloud air descends, i.e. W<0 within cloud body (Schmeisner et al. 2015). The subsiding dramatically decreases RH and leads to droplet evaporation. It is natural, that small droplets evaporate first. This decreases the life time of clouds in polluted air. It would be important to separate two effects: turbulent mixing of clouds with surrounding and their evaporation at W<0. Note that small Cu often dissipate and evaporate within the inversion layer, where turbulence (i.e. mixing is weak). In such case, namely subsiding place dominating role in cloud dissolving.

SA14) The aforementioned line raises the point that once dissipation commences the only method of cloud volume growth is by dilution via mixing with the environment. If precipitation below the LCL (lifting condensation level) is excluded, this dilution can only be attributed to mixing and not subsidence.

SC15) line 295. Which effect? How can precipitation be considered as a method of...? please reword the sentence. What kind of expansion can be induced by precipitation? Why the "choice to focus on volume above initial cloud base excludes this effect"? If the precipitation-induced cooling leads to the formation of new clouds, it is impossible to exclude the effect by the choice of the altitude, above which cloud properties are considered.

SA15) Continuing the previous answer (SA14), we wanted to differentiate between cloud volume expansions due to dilution versus cloud volume expansion due to precipitation below the cloud base. Since we have significant precipitation in the clean case, cloud mass descends below the initial cloud base (approximately the LCL) and increases the cloud volume significantly. For better comparison with the other more polluted cases, we took only the cloudy pixels above the initial cloud base (which is equal for all simulations) and thus volume changes can be attributed to other effects than precipitation below the cloud base.

SC16) line 295 Detrainment is the outflow of cloud mass from the cloud. It cannot change the cloud properties. Entrainment of dry environment air into the cloud indeed can lead to subsaturation. Regular (non-turbulent) entrainment takes place near cloud base. At later cloud edges lateral turbulent entrainment and mixing takes place.
SA16) Please see SA2 on this issue. We define detrainment as the opposite of entrainment (i.e. air flowing out of cloud). The outflow of air from the cloud can then mix with the surrounding similarly to when air is entrained into a cloud and mixes.

SC17) line 298. The effect of dilution depends on cloud width. The larger width the lower the effect of lateral mixing is. The increase or decrease of cloud width depends also on LWC.
SA17) In this section we are comparing three axi-symmetric single clouds which initially have the exact same width. In line 298 we just want to illustrate that the effect of dilution occurs, meaning increase in cloud volume at the same time there is loss of cloud mass: "***A clear indication for dilution is seen in Fig. 3 where between 30 and 35 mins of simulation time both the clean and polluted clouds lose total mass but only the clean cloud increases in total volume***".

SC18) line 300. What is "detrainment growth"?
SA18) The sentence was changed slightly to read: "…***limited in horizontal growth by detrainment*** ". As explained above in SA14, SA15, and SA16, growth by detrainment is when clouds may expand in volume after cloudy air is mixed with surrounding environmental air and the droplets do not fully evaporate.

SC19) line 314. To define "diffusion efficiency".
SA19) See MA2 for the issue to defining diffusion efficiency. Specifically, in the mentioned line we removed this term and replaced with "slow diffusion".

SC20) line 327. It is interesting to see the RH (r) profiles in the humid shell around cloud. SA20) Calculating and presenting the RH(r) profiles in the humid shell around all (or a subset of) clouds requires an extensive analysis which is beyond the scope of this work. Moreover, our focus here is on in-cloud processes and cloud properties rather than the effects on the environment adjacent to the cloud. Nevertheless, we note the previous works showing RH(r) have been done, one of them by a member of our research group , showing the distance scale for which RH decreases to the environmental mean.

SC21) line 375. Do you suppose that dissipating clouds may contain dominating cores? How does it agree with observations?
SA21) As can be seen in Fig. 5, many of the dissipating branch clouds (both larger and smaller ones) can be core dominated, mostly for the Wcore definition but also for a small percentage of clouds using the Bcore definition. We define the dissipation branch according to the COG height so that most dissipating clouds have a cloud base above the LCL and may still be mostly with updrafts. As for observations, according to our knowledge, most observations are biased to larger clouds with cloud base near the LCL and not the smaller cloud fragment which occupy the cloudy layer. Nevertheless, although not for small cumulus clouds, studies have shown frequent Bcore in downdrafts (Igau et al., 1999; Wei et al., 1998).

SC22) Line 375. Figure 5 shows that simulations with low CCN concentration were performed for the case of 2000 m inversion altitude. Two other simulations were performed for 1500 m altitude. The clouds should be quite different geometrically and microphysically in such cases. How can such clouds be compared?
SA22) Please see MA1 on this issue. The simulations were initialized with the same profile (and same inversion base height) but evolved differently due to different microphysical effects of the clouds on the thermodynamic conditions. In Fig. 5 we present the thermodynamic conditions after 5 h of simulations because we want them to reflect the actual state during the simulation and not the initial state. These different thermodynamic conditions are among the aerosol effects on clouds that are only seen in cloud field simulations.

SC23) Line 417. 1) we see again that there the difference in the inversion level in the simulations. Higher clouds can have larger cloud cover and longer life time etc. 2) It is necessary to add to the figure caption the conditions corresponding to the rows and columns or refer notations in fig 5.

SA23) For (1), see MA1 and SA22 above explaining the different inversion level heights. For (2), we have added description to the figure caption: "***CvM space diagrams showing the pixel fractions of Bcore within RHcore (left column), Bcore within Wcore (middle column), and RHcore within Wcore (right column), for the clean (top row), intermediate (middle row), and polluted (bottom row) simulations.".***

SC24) Line 458. I still wonder, how weak downdraft can lead to the temperature of subsiding air higher than in surrounding. Such subsidence should be actually along the moist adiabat. Why the downdrafts should be week? It seems that subsidence accompanied by evaporation leads to cold pool that accelerates formation of new clouds. It seems that positive buoyancy in the area of weak downdraft is the results of horizontal mixing between warm zone with W>0 (with high buoyancy) and the cloud periphery.

SA24) A rigorous explanation for buoyant downdrafts in now added to revised manuscript (see SA10). Basically, theory shows that cloudy downdrafts follow a lapse rate more unstable than the environment, meaning that a level of neutral buoyancy is reached above the cloud base. Since downdrafts have negative vertical momentum during descent, they will "undershoot" the equilibrium level and become positively buoyant. We show that this effect is highly dependent on aerosol concentration since the evaporation rates (and thus determine the lapse rate of descent. As shown in PT1 (and explained in SA10), mixing between positively buoyant and negatively buoyant regions is unlikely to create positively buoyant mixed parcels.

SC25) line 531. One can suppose that many clouds are isolated even in the clean case. Why do you illustrate the clean case by merging clouds?

SA25) Section 4.3 in the paper deals with the different relative humidity seen in the clouds for different aerosol concentrations. As part of this analysis, in Fig. 9 we present cross-sections of the most massive clouds for each simulation. In line 531 we just explain to the reader than the most massive clean cloud is actually composed to two large clouds that merge together and are connected by a few pixels (as can be clearly seen in Fig. 9). We choose to mention this because this is very typical of the clean case and a characteristic worth knowing (in our opinion), where precipitation promotes cold pools and later significant merging. We also mention this in the beginning of Sect. 4.1: "***The clean simulation (25 cm^{-3}) shows two disconnected regions of cloud scatter: one which is adjacent to the adiabatic approximation and one of mainly small mass and high COG clouds. The former region includes both clouds during their growth stages (smaller masses, LWP < 10 g m^{-2}) and large precipitating entities (larger masses, LWP > 10 g m^{-2}) which form due to merging processes (Heiblum et al., 2016b).***", and later in that section: "***We note that the higher cloud masses reached by lower aerosol concentration simulation can be explained by cloud field organization effects due to precipitation (i.e. increased merging of clouds) rather than increased cloud condensation (Heiblum et al., 2016b; Seigel, 2014)***.".

SC26) Line 572. So, the formation of low RH is the result of averaging over wider layers which contain the inversion layer and layer below LCL. Please confirm.
SA26) Exactly, the large clouds' margin regions may include areas in the inversion layer and layer below the LCL, and thus we may get low mean margin RH.

SC27) Line 619. Term convection is not suitable. Besides, if you want to compare T with surrounding, moist adiabatic cooling results in heating as compared with the surrounding.
SA27) In the revised manuscript we have changed the terms of the two positive buoyancy production processes to updraft buoyancy production and downdraft buoyancy production.

SC28) Line 621. Adiabatic heating is also not exact term. In the situation considered adiabatic heating is accompanied by turbulent mixing and droplet evaporation. So, many factors determine T in this area, so process is not adiabatic.
SA28) Thank you for this comment, it is true that a cloudy downdraft will likely not descend purely adiabatically. As described in the revised manuscript (and SA10), the descent of a cloudy parcel (during entrainment) will be following a lapse rate somewhere between the moist adiabat and dry adiabat, which represent the two extreme cases. We have removed the term "adiabatic heating" from the revised text.

References

Altaratz, O., Koren, I., Reisin, T., Kostinski, A., Feingold, G., Levin, Z. and Yin, Y.: Aerosols’ influence on the interplay between condensation, evaporation and rain in warm cumulus cloud, Atmos. Chem. Phys., 8(1), 15–24, doi:10.5194/acp-8-15-2008, 2008.

Andreae, M. O., Rosenfeld, D., Artaxo, P., Costa, A. A., Frank, G. P., Longo, K. M. and Silva-Dias, M. A. F.: Smoking rain clouds over the Amazon., Science, 303(5662), 1337–1342, doi:10.1126/science.1092779, 2004.

Betts, A. K.: Non-precipitating cumulus convection and its parameterization, Q.J Royal Met. Soc., 99(419), 178–196, doi:10.1002/qj.49709941915, 1973.

Betts, A. K.: Saturation point analysis of moist convective overturning, J. Atmos. Sci., 39(7), 1484–1505, doi:10.1175/1520-0469(1982)039<1484:SPAOMC>2.0.CO;2, 1982.

Betts, A. K. and Silva Dias, M. F.: Unsaturated downdraft thermodynamics in cumulonimbus, J. Atmos. Sci., 36(6), 1061–1071, doi:10.1175/1520-0469(1979)036<1061:UDTIC>2.0.CO;2, 1979.

Carrió, G. G. and Cotton, W. R.: On the buffering of CCN impacts on wintertime orographic clouds: An idealized examination, Atmos. Res., 137, 136–144, doi:10.1016/j.atmosres.2013.09.011, 2014.

Dagan, G., Koren, I. and Altaratz, O.: Competition between core and periphery-based processes in warm convective clouds – from invigoration to suppression, Atmos. Chem. Phys., 15(5), 2749–2760, doi:10.5194/acp-15-2749-2015, 2015.

Dagan, G., Koren, I., Altaratz, O. and Heiblum, R. H.: Aerosol effect on the evolution of the thermodynamic properties of warm convective cloud fields., Sci. Rep., 6, 38769, doi:10.1038/srep38769, 2016.

Dawe, J. T. and Austin, P. H.: Statistical analysis of an LES shallow cumulus cloud ensemble using a' ' cloud tracking algorithm, Atmos. Chem. Phys., 12(2), 1101–1119, doi:10.5194/acp-12-1101-2012, 2012.

de Roode, S. R. and Bretherton, C. S.: Mass-Flux Budgets of Shallow Cumulus Clouds, J. Atmos. Sci., 60(1), 137–151, doi:10.1175/1520-0469(2003)060<0137:MFBOSC>2.0.CO;2, 2003.

de Roode, S. R., Siebesma, A. P., Jonker, H. J. J. and de Voogd, Y.: Parameterization of the vertical velocity equation for shallow cumulus clouds, Mon. Wea. Rev., 140(8), 2424–2436, doi:10.1175/MWR-D-11-00277.1, 2012.

Garstang, M. and Betts, A. K.: A review of the tropical boundary layer and cumulus convection: structure, parameterization, and modeling, Bull. Amer. Meteor. Soc., 55(10), 1195–1205, doi:10.1175/1520-0477(1974)055<1195:AROTTB>2.0.CO;2, 1974.

Glassmeier, F. and Lohmann, U.: Precipitation Susceptibility and Aerosol Buffering of Warm- and Mixed-Phase Orographic Clouds in Idealized Simulations, J. Atmos. Sci., 75(4), 1173–1194, doi:10.1175/JAS-D-17-0254.1, 2018.

Grant, A. L. M. and Lock, A. P.: The turbulent kinetic energy budget for shallow cumulus convection, Q.J Royal Met. Soc., 130(597), 401–422, doi:10.1256/qj.03.50, 2004.

Grant, L. D. and van den Heever, S. C.: Cold pool and precipitation responses to aerosol loading: modulation by dry layers, J. Atmos. Sci., 72(4), 1398–1408, doi:10.1175/JAS-D-14-0260.1, 2015.

Heiblum, R. H., Altaratz, O., Koren, I., Feingold, G., Kostinski, A. B., Khain, A. P., Ovchinnikov, M., Fredj, E., Dagan, G., Pinto, L., Yaish, R. and Chen, Q.: Characterization of cumulus cloud fields using trajectories in the center of gravity versus water mass phase space: 1. Cloud tracking and phase space description, J. Geophys. Res. Atmos., 121(11), 6336–6355, doi:10.1002/2015JD024186, 2016a.

Heiblum, R. H., Altaratz, O., Koren, I., Feingold, G., Kostinski, A. B., Khain, A. P., Ovchinnikov, M., Fredj, E., Dagan, G., Pinto, L., Yaish, R. and Chen, Q.: Characterization of cumulus cloud fields using trajectories in the center of gravity versus water mass phase space: 2. Aerosol effects on warm convective clouds, J. Geophys. Res. Atmos., 121(11), 6356–6373, doi:10.1002/2015JD024193, 2016b.

Heus, T. and Jonker, H. J. J.: Subsiding Shells around Shallow Cumulus Clouds, J. Atmos. Sci., 65(3), 1003–1018, doi:10.1175/2007JAS2322.1, 2008.

Heus, T., Jonker, H. J. J., Van den Akker, H. E. A., Griffith, E. J., Koutek, M. and Post, F. H.: A statistical approach to the life cycle analysis of cumulus clouds selected in a virtual reality environment, J. Geophys. Res., 114(D6), doi:10.1029/2008JD010917, 2009.

Heus, T. and Seifert, A.: Automated tracking of shallow cumulus clouds in large domain, long duration large eddy simulations, Geosci. Model Dev., 6(4), 1261–1273, doi:10.5194/gmd-6-1261-2013, 2013.

Igau, R. C., LeMone, M. A. and Wei, D.: Updraft and downdraft cores in TOGA COARE: why so many buoyant downdraft cores?, J. Atmos. Sci., 56(13), 2232–2245, doi:10.1175/1520-0469(1999)056<2232:UADCIT>2.0.CO;2, 1999.

Jaenicke, R.: 9.3.1 Physical properties, in Physical and chemical properties of the air, edited by G. Fischer, pp. 405–420, Springer-Verlag, Berlin/Heidelberg., 1988.

Khairoutdinov, M. F., Krueger, S. K., Moeng, C.-H., Bogenschutz, P. A. and Randall, D. A.: Large-eddy simulation of maritime deep tropical convection, J. Adv. Model. Earth Syst., 2, 15, doi:10.3894/JAMES.2009.1.15, 2009.

Knupp, K. R. and Cotton, W. R.: Convective cloud downdraft structure: An interpretive survey, Rev. Geophys., 23(2), 183, doi:10.1029/RG023i002p00183, 1985.

Kogan, Y. L. and Martin, W. J.: Parameterization of bulk condensation in numerical cloud models, J. Atmos. Sci., 51(12), 1728–1739, doi:10.1175/1520-0469(1994)051<1728:POBCIN>2.0.CO;2, 1994.

Köhler, H.: The nucleus in and the growth of hygroscopic droplets, Transactions of the Faraday Society, 32, 1152–1161, 1936.

Koren, I., Dagan, G. and Altaratz, O.: From aerosol-limited to invigoration of warm convective clouds., Science, 344(6188), 1143–1146, doi:10.1126/science.1252595, 2014.

Kumar, V. V., Jakob, C., Protat, A., Williams, C. R. and May, P. T.: Mass-Flux Characteristics of Tropical Cumulus Clouds from Wind Profiler Observations at Darwin, Australia, J. Atmos. Sci., 72(5), 1837–1855, doi:10.1175/JAS-D-14-0259.1, 2015.

Lebo, Z. J. and Seinfeld, J. H.: Theoretical basis for convective invigoration due to increased aerosol concentration, Atmos. Chem. Phys., 11(11), 5407–5429, doi:10.5194/acp-11-5407-2011, 2011.

Mason, B. J. and Chien, C. W.: Cloud-droplet growth by condensation in cumulus, Quarterly Journal of the Royal Meteorological Society, 88(376), 136–142, 1962.

Morrison, H.: On the robustness of aerosol effects on an idealized supercell storm simulated with a cloud system-resolving model, Atmos. Chem. Phys., 12(16), 7689–7705, doi:10.5194/acp-12-7689-2012, 2012.

Neggers, R. A. J., Stevens, B. and Neelin, J. D.: Variance scaling in shallow-cumulus-topped mixed layers, Q.J Royal Met. Soc., 133(628), 1629–1641, doi:10.1002/qj.105, 2007.

Paluch, I. R. and Breed, D. W.: A Continental Storm with a Steady, Adiabatic Updraft and High Concentrations of Small Ice Particles: 6 July 1976 Case Study, J. Atmos. Sci., 41(6), 1008–1024, doi:10.1175/1520-0469(1984)041<1008:ACSWAS>2.0.CO;2, 1984.

Reutter, P., Su, H., Trentmann, J., Simmel, M., Rose, D., Gunthe, S. S., Wernli, H., Andreae, M. O. and Pöschl, U.: Aerosol- and updraft-limited regimes of cloud droplet formation: influence of particle number, size and hygroscopicity on the activation of cloud condensation nuclei (CCN), Atmos. Chem. Phys., 9(18), 7067–7080, doi:10.5194/acp-9-7067-2009, 2009.

Romps, D. M. and Charn, A. B.: Sticky Thermals: Evidence for a Dominant Balance between Buoyancy and Drag in Cloud Updrafts, J. Atmos. Sci., 72(8), 2890–2901, doi:10.1175/JAS-D-15-0042.1, 2015.

Saleeby, S. M., Herbener, S. R., van den Heever, S. C. and L'Ecuyer, T.: Impacts of cloud droplet–nucleating aerosols on shallow tropical convection, J. Atmos. Sci., 72(4), 1369–1385, doi:10.1175/JAS-D-14-0153.1, 2015.

Savane, O., Vant-Hull, B., Mahani, S. and Khanbilvardi, R.: Effects of aerosol on cloud liquid water path: statistical method a potential source for divergence in past observation based correlative studies, Atmosphere, 6(3), 273–298, doi:10.3390/atmos6030273, 2015.

Seifert, A., Heus, T., Pincus, R. and Stevens, B.: Large-eddy simulation of the transient and near-equilibrium behavior of precipitating shallow convection, J. Adv. Model. Earth Syst., 7(4), 1918–1937, doi:10.1002/2015MS000489, 2015.

Seigel, R. B.: Shallow Cumulus Mixing and Subcloud-Layer Responses to Variations in Aerosol Loading, J. Atmos. Sci., 71(7), 2581–2603, doi:10.1175/JAS-D-13-0352.1, 2014.

Sheffield, A. M., Saleeby, S. M. and van den Heever, S. C.: Aerosol-induced mechanisms for cumulus congestus growth, J. Geophys. Res. Atmos., 120(17), 8941–8952, doi:10.1002/2015JD023743, 2015.

Siebesma, A. P. and Cuijpers, J. W. M.: Evaluation of parametric assumptions for shallow cumulus convection, J. Atmos. Sci., 52(6), 650–666, doi:10.1175/1520-0469(1995)052<0650:EOPAFS>2.0.CO;2, 1995.

Stevens, B. and Feingold, G.: Untangling aerosol effects on clouds and precipitation in a buffered system., Nature, 461(7264), 607–613, doi:10.1038/nature08281, 2009.

Storer, R. L. and van den Heever, S. C.: Microphysical processes evident in aerosol forcing of tropical deep convective clouds, J. Atmos. Sci., 70(2), 430–446, doi:10.1175/JAS-D-12-076.1, 2013.

Twomey, S.: The influence of pollution on the shortwave albedo of clouds, J. Atmos. Sci., 34(7), 1149–1152, doi:10.1175/1520-0469(1977)034<1149:TIOPOT>2.0.CO;2, 1977.

Wei, D., Blyth, A. M. and Raymond, D. J.: Buoyancy of convective clouds in TOGA COARE, J. Atmos. Sci., 55(22), 3381–3391, doi:10.1175/1520-0469(1998)055<3381:BOCCIT>2.0.CO;2, 1998.

Xu, K.-M. and Randall, D. A.: Updraft and downdraft statistics of simulated tropical and midlatitude cumulus convection, J. Atmos. Sci., 58(13), 1630–1649, doi:10.1175/1520-0469(2001)058<1630:UADSOS>2.0.CO;2, 2001.

Zhao, M. and Austin, P. H.: Life cycle of numerically simulated shallow cumulus clouds. part I: transport, J. Atmos. Sci., 62(5), 1269–1290, doi:10.1175/JAS3414.1, 2005a.

Zhao, M. and Austin, P. H.: Life cycle of numerically simulated shallow cumulus clouds. part II: mixing dynamics, J. Atmos. Sci., 62(5), 1291–1310, doi:10.1175/JAS3415.1, 2005b.

Core and margin in warm convective clouds. Part II: aerosol effects on core properties

[1]Reuven H. Heiblum, [1]Lital Pinto, [1]Orit Altaratz, ~~[1]Guy~~[1,2]Guy Dagan, [1]Ilan Koren

[1]Department of Earth and Planetary Sciences, Weizmann Institute of Science, Rehovot, Israel

[2]now at: Atmospheric, Oceanic and Planetary Physics, Department of Physics, University of Oxford, UK

Corresponding Email – ilan.koren@weizmann.ac.il

Abstract:

The effects of aerosol on warm convective cloud cores are evaluated using single cloud and cloud field simulations. Three core definitions are examined: positive vertical velocity (Wcore), supersaturation (RHcore), and positive buoyancy (Bcore). As presented in Part I, the property Bcore $\subset$ RHcore $\subset$ Wcore is seen during growth of warm convective clouds. We show that this property is kept irrespective of aerosol concentration. During dissipation core fractions generally decrease with less overlap between cores. However, for clouds that develop in low aerosol concentrations capable of producing precipitation, Bcore and subsequently Wcore volume fractions may increase during dissipation (i.e. loss of cloud mass). The RHcore volume fraction decreases during cloud lifetime and shows minor sensitivity to aerosol concentration.

It is shown that a Bcore forms due to two processes: i) ~~Convection~~ Convective updrafts – condensation within supersaturated updrafts and release of latent heat, ii) ~~Adiabatic heating due to weak~~Dissipative downdrafts – sub-saturated cloudy downdrafts that warm during descent “undershoot” the level of neutral buoyancy. The former process occurs during cloud growth for all aerosol concentrations. The latter process only occurs for low aerosol concentrations during dissipation and precipitation stages where large mean drop sizes permit slow evaporation rates~~.~~ and sub-saturation during descent.

The aerosol effect on the diffusion efficiencies play a crucial role in the development of the cloud and its partition to core and margin. Using the RHcore definition, it is shown that the total cloud mass is mostly dictated by core processes, while the total cloud volume is mostly dictated by margin processes. Increase in aerosol concentration increases the core (mass and volume) due to enhanced condensation but also decreases the margin due to evaporation. In clean clouds larger droplets evaporate much slower, enabling preservation of cloud ~~volume~~size and even increase by ~~dilution (~~detrainment and dilution (volume increase while losing mass). This explains how despite having smaller cores and less mass, cleaner clouds may live longer and grow to larger sizes.

1. Introduction

Aerosols remain one of the largest sources of uncertainty in climate predictions, mainly via their effects on clouds (IPCC, 2013). Here we focus on the aerosol effects on warm clouds. Aerosols act as cloud condensation nuclei (CCN) during heterogeneous nucleation ~~by reducing the supersaturation required for droplet activation~~of cloud droplets (Köhler, 1936; Mason and Chien, 1962)~~, yielding~~. The number, size, and composition of aerosol distribution yields differences in the initial cloud droplet size distribution (DSD). Polluted clouds (i.e. more aerosols) have more, but smaller droplets, and a narrower DSD compared to clean clouds (Andreae et al., 2004; Twomey, 1977). Changes in the initial DSD drive various effects and feedbacks on the cloud's evolution and key processes, such as: droplet mobility, condensation/evaporation budgets, collision-coalescence, and entrainment (Jiang et al., 2006; Koren et al., 2015; Small et al., 2009; Xue and Feingold, 2006).

It is well known that an abundance of small droplets in a cloud (a narrow DSD) reduces the efficiency of the collision-coalescence process (Squires, 1958; Twomey, 1977; Warner, 1968), prolongs the diffusional growth time (Khain et al., 2005; Wang, 2005), and delays or even completely suppresses the initiation of precipitation (Albrecht, 1989; Hudson and Mishra, 2007; Hudson and Yum, 2001; L'Ecuyer et al., 2009). Moreover, in-cloud condensational growth is more efficient in consuming supersaturation because of the larger surface area-to-volume ratio of droplets (Dagan et al., 2015a, 2015b; Mordy, 1959; Pinsky et al., 2013; Reutter et al., 2009; Seiki and Nakajima, 2014). ~~These processes~~We note that throughout this work the word *efficient* will be used to describe both the rate and the total change of mass attributed to a microphysical process. The processes described above enable the more polluted cloud to condense more water and intensify its growth via increased release of latent heat (Kogan and Martin, 1994; Koren et al., 2014; Saleeby et al., 2015; Sheffield et al., 2015). The smaller droplets are also pushed higher in the atmosphere due to larger droplet mobility (Koren et al., 2014, 2015).

However, the increase in aerosol amount yields suppressing effects as well. ~~The symmetry of the diffusion equation dictates that an~~An opposite effect should take place in the sub saturated regions of the cloud, where more numerous and smaller droplets increase the evaporation rate and loss of cloud mass (Grant and van den Heever, 2015; Saleeby et al., 2015; Storer and van den Heever, 2013). Henceforth evaporation will be referred to as a process (i.e. change of mass per unit time) rather than complete evaporation of a water drop. Increased evaporation can promote entrainment mixing which in turn mixes more sub saturated air into the cloud and further promotes evaporation (Jiang et al., 2006; Small et al., 2009; Xue and Feingold, 2006), effectively initiating a positive feedback between evaporation and mixing with the eventual suppression of cloud growth. This effect may also be accompanied by a suppressing effect of the larger water loading in polluted clouds which contain more liquid water mass.

The competition between those opposing processes that are driven by enhanced aerosol loading determines the net aerosol effect on cloud properties such as cloud fraction, lifetime, albedo, mass, size, and precipitation amount. However, the sign and magnitude of such effects are non-trivial (Jiang and Feingold, 2006). Previous studies report opposing findings regarding the total aerosol effects on warm clouds (Altaratz et al., 2014). Some studies suggest cloud invigoration by aerosols (bigger and deeper clouds) (Dey et al., 2011; Kaufman et al., 2005; Koren et al., 2014; Yuan et al., 2011) while some suggest cloud suppression or no effect at all (Jiang and Feingold, 2006; Li et al., 2011; Savane et al., 2015; Xue et al., 2008). Moreover, other work has shown that the precipitation susceptibility (i.e. quantifies the sensitivity of precipitation to the aerosol increase) has a non-monotonic behavior that reaches its maximum at intermediate LWP values (Sorooshian et al., 2009), implying that the resultant aerosol effects are heavily dependent on cloud type and environmental conditions (Khain et al., 2008)~~. (Stevens and Feingold, 2009) (Carrió and Cotton, 2014; Glassmeier and Lohmann, 2018; Seifert et al., 2015)~~.

~~A unified theory for the contradicting results regarding aerosol effects~~A different approach to aerosol effects suggests that cloud systems can be buffered to microphysical effects (Stevens and Feingold, 2009). Several studies have shown that given enough time for the cloud system to reach steady state, cloud macro-physical parameters (e.g. cloud fraction, rain yield) show similar results for various aerosol concentrations (Carrió and Cotton, 2014; Glassmeier and Lohmann, 2018; Seifert et al., 2015). Based on the idea that clouds can be partitioned to aerosol-limited, updraft-limited, or aerosol and updraft sensitive regimes (Reutter et al., 2009), a unified theory for the contradicting results regarding aerosol effects was suggested (Dagan et al., 2015b)~~was shown in recent work (Dagan et al., 2015b). It was shown that~~. Given an aerosol range that covers all three regimes, the competition between opposite processes leads to an optimum value of aerosol concentration regarding various cloud properties like total mass, cloud top, or rain (Dagan et al., 2015b). A cloud that develops under low aerosol concentration is aerosol limited, as it does not have enough collective droplet surface area to consume the available water vapor. On the other side of the trend, a cloud that develops in polluted environment (with more aerosols than the optimum) is influenced significantly by enhanced entrainment and larger water loading, causing suppression of cloud development. The optimal concentration is a function of the thermodynamic conditions (temperature and humidity profiles) and cloud size.

Environments that support larger clouds development will have larger cloud cores that are positively affected by aerosol increase and can be regarded as aerosol limited (i.e. on the ascending branch of the aerosol trend) up to a higher optimal aerosol concentration. Environmental conditions that support small clouds are more strongly affected by cloud suppression processes at the cloud margins (due to higher cloud surface area to volume ratio) and would have a lower optimal aerosol concentration. This can explain why studies biased to smaller clouds (mostly numerical modeling studies) report cloud suppression and studies biased to larger clouds (mostly observational studies) report cloud invigoration. Similar conclusions were reached for the cloud field scale as well (Dagan et al., 2017).

In addition, it was shown that clouds impact differently the environmental thermodynamics according to the aerosol level in the field (Dagan et al., 2016; Seifert and Heus, 2013; Seifert et al., 2015). For example changes in aerosol loading impact the amount of precipitation reaching the surface and subsequently the evaporative cooling below cloud base and the organization patterns (Seifert and Heus, 2013; Seigel, 2014; Xue et al., 2008). Moreover, an increase in aerosol loading may increase evaporation rates around the margins and tops of clouds (Seigel, 2014; Stevens, 2007; Xue and Feingold, 2006), cooling the upper cloudy layer and increasing the convective instability. Therefore aerosol effects on phase changes and precipitation result in vertical redistribution of heat and moisture, which may either stabilize or destabilize the environment in which subsequent clouds grow (Seifert and Heus, 2013).

Irrespective of the definition chosen, the cloud's core and margin are dominated by different processes (Dagan et al., 2015b). These processes often compete with each other, with the dominant one changing along the cloud's evolution. For example, at the initial stage of cloud formation, a cloud is more adiabatic and is controlled by the core's processes (condensation), and when it dissipates the margin processes are more dominant (entrainment and evaporation). Aerosols affect each of these processes and thus each stage in the cloud's lifetime. As a continuation to Part I of this work (hereafter PTI), in this part we analyze aerosols effects on the cloud's partition to core and margin throughout the lifetime of a cloud. We report the consequences these effects have on evolution of a cloud, in terms of volume, mass, and lifetime. As opposed to other works that typically focus on a single cloud core definition, here three different definitions are used (see Sect. 2), with emphasis put on the sensitivity of each core definition to aerosol concentration. Moreover, the combination of single cloud with large eddy simulations enables us to gain process level understanding and test the robustness of our findings.

2. Methods

The analyses performed here are to the most part identical to those described in ~~Part I~~PTI of this work. In this section we shall thus only give a brief review of the methods used. For single cloud simulations we use the Tel-Aviv University axisymmetric cloud model (TAU-CM (Reisin et al., 1996)), and for cloud field simulations we use the System for Atmospheric Modeling (SAM) Model (version 6.10.3, for details see webpage: http://rossby.msrc.sunysb.edu/~marat/SAM.html, (Khairoutdinov and Randall, 2003)).

Both models utilize explicit bin microphysics schemes (Khain et al., 2004; Tzivion et al., 1987), solving nucleation, diffusion (i.e. condensation and evaporation), collisional coalescence, breakup, and sedimentation microphysical processes. The single cloud model is initialized using a Hawaiian thermodynamic profile, based on the 91285 PHTO Hilo radiosonde at 00Z, 21 Aug, 2007. The cloud field model is setup based on the BOMEX case study, including an initialization setup (sounding, surface fluxes, and surface roughness) and large scale forcing setup (Siebesma et al., 2003). More details on the model setups and definitions can be found in PTI.

To study the effects of aerosols on the cloud cores we run each model setup with three different aerosol concentrations: clean – 25 cm^{-3}, intermediate – 250 cm^{-3}, and polluted – 2000 cm^{-3}~~.(Heiblum et al., 2016a) As defined in Part I~~. The model domain is initialized using an oceanic size distribution (Altaratz et al., 2008; Jaenicke, 1988), maintaining constant mixing ratio with height. Aerosol budget includes removal by nucleation and regeneration upon evaporation, while wet scavenging by precipitation removes aerosols from the domain. Thus, the aerosol concentration may be depleted by 20%–40% (depending on the precipitation amount) during the simulation. More on the treatment of aerosols in the cloud field model can be found in previous work (Heiblum et al., 2016a). As defined in PTI, all pixels with at least 0.01 g kg^{-1} of liquid water are considered cloudy. Cloud cores are defined using three definitions: -1) RHcore: relative humidity > 100%, 2) ~~B_{core}:~~Bcore: buoyancy > 0, and 3) ~~W_{core}:~~Wcore: vertical velocity > 0. Relative humidity (RH) and vertical velocity (W) are standard outputs of the model, while the buoyancy (B) is calculated based on eq. 1 in PTI, where each cloudy pixel is compared with the mean non-cloudy thermodynamic reference state per height.

In order to reduce the problem’s dimensionality and distill signals in a cloud field system governed by high variance, we use the Gravity vs. Mass (CvM) phase space in combination with an automated 3D cloud tracking algorithm (Heiblum et al., 2016a). The CvM phase space enables a compact view of all clouds in the simulation, by projecting only their Center-of-Gravity (COG) height and mass at each output time step. Using the cloud tracking, it was shown that the lifetime of a cloud can be described by a trajectory on this phase space. Hence, the different locations in the CvM space are associated with different stages in a cloud's lifetime (i.e. growing, precipitating, and dissipating). For an in-depth explanation of the CvM space, the reader is referred to Sect. 2.4 in PTI (see schematic illustration - Fig. 1, PTI).

3. Results – Single cloud simulations

3.1. Sensitivity of different core types to aerosol concentration

Figure 1 presents time series of single cloud core volume fractions and cores' properties, for three aerosol concentrations (clean, intermediate, and polluted). Also included are time series of instantaneous rain-rates [mm hr^{-1}] at the domain surface. For all aerosol concentrations and during most of the clouds' lifetimes, the volume fraction of ~~W_{core}~~Wcore tends to be the largest and of ~~B_{core}~~ Bcore the smallest. Exceptions to this finding are seen either at the initial time step for the polluted cloud or the later stages of cloud lifetime for the lower concentration clouds. In addition, we find that ~~$RH_{core} \subseteq W_{core}$~~RHcore ⊂ Wcore for all stages of cloud lifetime while ~~$B_{core} \subseteq W_{core}, RH_{core}$~~Bcore ⊂ Wcore, RHcore for all stages of the polluted cloud but only applies to the growing stages of lower concentration clouds before precipitation production. Thus, the main finding from PTI (i.e. ~~$B_{core} \subseteq RH_{core} \subseteq W_{core}$)~~Bcore ⊂ RHcore ⊂ Wcore) generally applies to all aerosol concentrations during the pre-precipitation stages of the clouds' lifetimes.

Lower aerosol concentration simulations produce more rain, and at earlier stages of cloud lifetime due to efficient collision coalescence. The increase in ~~B_{core}~~Bcore volume fraction at later stages of cloud lifetime in those simulations (clean and intermediate) coincides with initiation of precipitation production, followed by a consequent increase in ~~W_{core}~~Wcore volume fraction as well (more so for the intermediate concentration). This dissipating Wcore is mostly contained within the Bcore. The possible mechanism behind the increase in prevalence of buoyant parcels during precipitation is explored in Sect. 3.2. The lack of ~~RH_{core}~~RHcore pixels at these stages indicates that the ~~W_{core}~~Wcore is composed of pixels with small vertical velocities, insufficient for supersaturation production. The ~~RH_{core}~~RHcore is the only one which is not sensitive to rain and monotonically decreases during all clouds' lifetimes. Another clear aerosol effect seen in Fig. 1 is an increase in cloud lifetime with decrease in aerosol concentration. This point will be further explored in Sect. 3.3.

3.2. Mechanisms governing positive buoyancy

The theoretical arguments in PTI showed that ~~B_{core}~~Bcore should be the smallest of the three. This was shown for both the adiabatic cloud column case and also the non-adiabatic case where entrainment mixing and consequent evaporation has a strong net negative effect has on cloud buoyancy. Despite this fact, results show (see Fig. 1, and Fig. 2 in PTI) that pockets of positive buoyancy may form independent of the other cores during dissipation and precipitation stages, even though evaporation is to be expected then. Since positive buoyancy is the result of either higher temperature or vapor content (or both) than the surrounding environment, we choose to analyze these two terms during different stages of the single ~~cloud lifetimes.~~clouds' lifetimes. The liquid water content buoyancy term (not shown here) is always negative and typically increases (in absolute value) with increase in vertical velocity or total buoyancy.

Figure 2 shows the values of the temperature (B_T) and humidity (B_{Qv}) buoyancy terms in pixel buoyancy vs. pixel vertical velocity phase space. The scatter plots include all cloudy pixels during all time steps, for the three different aerosol concentration simulations. The distribution of points for the polluted simulation shows a positive linear dependence of buoyancy on vertical velocity. Negative vertical velocity is associated with negative buoyancy and positive vertical velocity shows a transition from negative to positive buoyancy with increase in magnitude. For this case both B_T and B_{Qv} increase with increase in vertical velocity, as is generally expected in convective clouds. The sign of pixel buoyancy is mostly dependent on B_T since all pixels have positive B_{Qv} and a negative water loading term. This behavior is also seen for lower aerosol concentrations, where the sign of buoyancy is to the most part determined by B_T. Hereafter, we refer to positive buoyancy (both B_T and B_{Qv}) production within updrafts as updraft buoyancy.

The clean and intermediate simulations show a similar dependence of buoyancy on vertical velocity; however, it is apparent that these simulations also include an outlier scatter region of pixels with positive buoyancy and weak negative vertical velocity which is absent in the polluted simulation (see white arrows, Fig. 2). Consistent with the rest of the cloudy pixels, these outlier pixels have positive B_T, but differ in that they show neutral B_{Qv}. It can also be seen that these pixels are only attributed to the stages after surface precipitation has commenced (indicated by black dots in markers). Precipitation is indicative of both downdraft motion and abundance of large ~~droplet~~drop sizes.

~~Thus, we hypothesize that pockets of positive buoyancy may form due to transport of parcels with higher potential temperature from above, namely adiabatic heating. The weak downdrafts also transport lower mixing ratio (Q_v) values, as is indicated by the neutral B_{Qv}.~~Although not usually the focus of studies, the existence of positively buoyant downdrafts in convective clouds has been reported in both observations (Igau et al., 1999; Wei et al., 1998) and simulations (Xu and Randall, 2001; Zhao and Austin, 2005a, 2005b). A possible explanation for this can be deduced from previous theoretical studies predicting mixing induced downdrafts in cumulus clouds (Betts and Silva Dias, 1979; Betts, 1982). It was shown that in some cases cloud - environment mixtures are negatively buoyant (while still containing liquid water) and the consequent downdrafts can sometimes descend only part way down to the cloud base before reaching neutral buoyancy. Similar to convective overshooting, parcels with negative vertical momentum may then “undershoot” the downdraft equilibrium level and turn positively buoyant while the downdraft weakens. One can therefore expect the magnitude of positive buoyancy within the downdraft to reach a maximum when the velocity approaches zero. Hereafter we refer to positive buoyancy production within downdrafts as downdraft buoyancy.

Downdraft buoyancy production occurs frequently in cumulus fields because the negatively buoyant downdrafts follow a warming lapse rate which is more unstable than the environmental one, which is typically between the dry adiabat and moist adiabat (as is the case for the Hawaiian and BOMEX profiles simulated in this work). On one extreme, a descending parcel is least buoyant (i.e. coolest) when evaporation (after mixing) keeps it just barely saturated (Paluch and Breed, 1984, also PTI) so that the lapse rate of descent tends to moist adiabatic and may remain negatively buoyant. On the other extreme, if little to no evaporation of liquid water occurs, the descent will follow the dry adiabat and switch to neutral (and then positive) buoyancy rapidly. Thus, the ability of a negatively buoyant cloudy downdraft to sustain itself depends on continuous inflow of liquid water (by mixing) and its consequent evaporation (Knupp and Cotton, 1985).

Indeed, the results in Fig. 2 match the hypothesis explained above, where positively buoyant downdrafts are warmer than the environment, and tend to show larger buoyancy values for weaker downdrafts velocities (especially for the intermediate case). Further analysis also shows that the more unsaturated the downdrafts (indicated also by low B_{Qv}), the larger the positive buoyancy. Moreover, the occurrence during precipitating stages and for lower aerosol concentrations indicates that slow evaporation due to larger ~~droplet sizes is crucial. Indeed, most pixels with negative buoyancy show positive B_{Qv} except for the clean case where rain pixels from the cloudy layer sediment well below the cloud base and experience higher environmental Qv (while evaporating slowly), resulting in negative B_{Qv}.~~drop sizes is crucial for downdraft buoyancy production, enabling a near dry adiabatic lapse rate during descent.

3.3. The dependency of cloud characteristics on core and margin's processes

Here we evaluate how aerosol effects within the core and margin (using the three core definitions) affect the cloud characteristics, focusing on two main parameters; size (or volume) and mass. In Fig. 3 we follow the evolution of cloud, core, and margin mass and volume for different aerosol concentrations, using only the ~~RH_{core}~~RHcore definition. We choose the ~~RH_{core}~~RHcore since it is the most well behaved out the core types, generally decreasing monotonically (see Fig. 1). A non-monotonic dependency of total cloud mass on aerosol concentration is seen, showing a maximum for the intermediate concentration. This type of dependency has been previously reported for warm cumulus clouds (Dagan et al., 2015b; Savane et al., 2015).

One can generally expect an increase in diffusion and decrease in collision-coalescence processes efficiency with increase in aerosol concentration (Hudson and Yum, 2001; Jiang et al., 2009; L'Ecuyer et al., 2009; Pinsky et al., 2013), affecting both condensation and evaporation processes. The intermediate concentration shows the highest total mass as a result of being an optimal case with higher condensation efficiency than the clean case and lower evaporation efficiency than the polluted case. It is convenient to represent the condensation and evaporation efficiencies by the ~~RH_{core}~~ RHcore and ~~RH_{margin}~~RHmargin mass, respectively. The intermediate cloud has almost identical core mass as does the polluted cloud, but retains higher mass in its margin as well. The clean cloud shows the lowest core mass but manages to accumulate the largest mass in its margin that dissipates slowly in ~~subsaturated~~sub-saturated conditions. By comparing the total cloud mass evolution with the core and margin mass evolutions, it becomes clear that the total mass is primarily dependent on the cloud core. Another way to see this is by plotting the core mass fraction (Fig. 3 bottom panel), which shows that clouds are core dominated (core fraction > 0.5) with respect to mass for most of their lifetimes, and for all aerosol concentrations.

With respect to cloud total volume, the lower the concentration, the larger the total cloud volume. We note that the cloud volume here excludes regions of precipitation below the initial cloud base height. By separating to core and margin regions, one can see that the total cloud volume is primarily dependent on the volume of the margin, which increases significantly with decreasing concentration. This is especially true during the dissipating stages of cloud lifetime, when the cloud is margin dominated. Although increasing the aerosol concentration does initially yield an increase in core volume (as was seen for the mass), the extents of the core size are typically smaller than those of the margin. There are large differences in the relative core volume percent for the different clouds. The clean (polluted) cloud is margin (core) dominated with respect to volume for most of its lifetime. Excluding time of formation, the clean cloud shows the lowest core volume fractions, but manages to maintain its core for the longest time span.

These results with respect to cloud volume can ~~again~~ be attributed to the smaller drop sizes and higher diffusion efficiencies with increase in aerosol concentration. Additionally, lower collision-coalescence efficiencies also maintain a narrow droplet spectrum of small droplets in the polluted cloud. During the growing stage a higher aerosol concentration may permit the cloud to condense more water, release more latent heat, and promote cloud growth. This explains the larger core volume sizes. However, after the cloud exhausts its convective potential (i.e. the growth of the convective core terminates and reaches its peak in mass), its main method of expansion is by mixing with the environment (i.e. detrainment and dilution). We note that precipitation can also be considered a method of expansion; however our choice to focus on volume above initial cloud base excludes this effect. ~~–~~Detrainment ~~results~~and mixing with the environment result in sub-saturation conditions and evaporation of LWC. A clear indication for dilution is seen in Fig. 3 where between 30 and 35 mins of simulation time both the clean and polluted clouds lose total mass but only the clean cloud increases in total volume. The polluted cloud is composed of small drops, evaporates its margin regions efficiently, and is thus limited in horizontal growth by detrainment ~~growth~~. The clean cloud is composed of larger drops, less efficient in evaporating its margins, and hence can grow by dilution of its LWC upon a larger volume. This large margin "shields" the core during dissipation stages and enables it to the live for a longer time.

The mechanism behind the results in Fig. 3 is demonstrated in Fig. 4, where horizontal cross-sections of mean (taken in the vertical dimension) cloud RH are shown for different stages during the clouds' lifetimes. For the polluted cloud, super- or sub-saturated conditions are rare. The RH throughout the cloud is near 100% (almost always between 99.8% and 100.2%) except for a few pixels at its far edges which are a bit below 99%. The polluted cloud resembles what one would expect to see using a moist adiabatic approximation (i.e. saturation adjustment), where all excess water vapor above saturation is converted to liquid water, mimicking infinitely efficient condensation (and evaporation).

The clean cloud shows opposite behavior, with extremes of large super-saturation during cloud growth (initial stages) and large sub-saturation during cloud dissipation (final stages). ~~Both extremes can be explained by the low diffusion efficiency in this case.~~The large super-saturation can be explained by slow diffusional growth, but the large sub-saturation also takes into consideration the larger drop sizes which take more time to evaporate. This enables the clean cloud to expand to larger horizontal extents (by dilution and mixing with the environment without fully evaporating) and live for longer times. The intermediate aerosol concentration shows a midway scenario, where the super-saturation is consumed more efficiently than the clean case and at the same time much larger values of sub-saturation may exist than those seen for the polluted case.

4. Results – Cloud field simulations

In the following section we expand our analyses of aerosol effects on cloud core and margin from the single cloud scale to the cloud field scale. A cloud field can be considered as composed of many individual clouds and thus can serve to test the robustness of the aerosol effects seen for a single cloud. Moreover, cloud fields include the added complexity of interactions between clouds and the clouds' effects on their thermodynamic environment.

4.1. Sensitivity of different core types to aerosol concentration

Here CvM space representations (see Sect. 2) are used to observe the core volume fractions of all clouds in BOMEX cloud field simulations. The rows in Fig. 5 represent different aerosol concentrations while the columns represent different core type definitions. Different aerosol concentrations produce a vastly different scatter of clouds in the CvM space, as was previously discussed in depth (Heiblum et al., 2016b). The clean simulation (25 cm^{-3}) shows two disconnected regions of cloud scatter: one which is adjacent to the adiabatic approximation and one of mainly small mass and high COG clouds. The former region includes both clouds during their growth stages (smaller masses, LWP < 10 g m^{-2}) and large precipitating entities (larger masses, LWP > 10 g m^{-2}) which form due to merging processes (Heiblum et al., 2016b). The latter region (small mass and high COG) includes clouds at their dissipating stage, which form by shedding mechanism off the large cloud entities. We note also the existence of small mass elements well below the adiabat, representing precipitation cloud segments which shed off large precipitating clouds.

The polluted simulation (2000 cm^{-3}) shows a much more homogeneous scatter of clouds. The lower part of the scatter (closest to the adiabat) represents the cloud growing branch while the rest of the scatter represents dissipating clouds, either by gradual process of rising cloud base or by immediate process of shedding off larger cloud entity (see Fig. 1, PTI). Precipitating cloud segments below the adiabat are absent from this simulation. The intermediate simulation (250 cm^{-3}) shows a scatter which generally more resembles the polluted case. However, the existence of relatively disconnected (from the main cloud scatter) small mass cloud segments below the adiabat and near the inversion base height resembles the clean simulation as well. ~~(Heiblum et al., 2016b)~~It should be noted that horizontal dashed lines in Fig. 5 represent the inversion base height after 5 hours of simulation (approximately middle of simulation), where an increase in the inversion base height is seen with decrease in aerosol concentration. This is due to increased net warming in the upper cloudy layer (i.e., release of latent heat during condensation with reduced local evaporation) with increase in precipitation (Dagan et al., 2016; Heiblum et al., 2016b), which raises the inversion base.

The results in Fig. 5 show a consistent behavior of the core volume fractions for all aerosol concentrations, where the ~~W_{core}~~Wcore type shows the largest fractions and the ~~B_{core}~~Bcore type shows the smallest fractions. The ~~W_{core}~~Wcore and ~~RH_{core}~~RHcore generally show a decrease in core fractions along the growing branch while the ~~B_{core}~~Bcore fraction initially increase with cloud growth and then decrease for the large mass growing clouds. The percentages in the panel legends (Fig. 5) indicate the fraction of clouds (out of the scatter) which are core dominated with respect to volume ($f_{vol} > 0.5$). For all concentrations, less than 7% of clouds are Bcore dominated while more than 55% are Wcore dominated (with RHcore percentages somewhere in between). The Bcore typically occupies a small portion of a typical cloud volume while the Wcore typically occupies most of the cloud. The mean cloud area (proportional to scatter point size) shows an increase with increase in mean clouds LWP.

These results are consistent with PTI and the single cloud simulations in Sect. 3.1. Nevertheless, some significant aerosol effects on the partition to core types can be seen. Focusing on the growing branch first (i.e. clouds located near the adiabat), we note the following:

1) For the ~~RH_{core}~~RHcore type, the core volume fractions of clouds after formation (i.e. with small mass) increase with decreasing aerosol concentration. This effect was also seen for the single cloud simulations and can be explained by the reduced efficiency of super-saturation consumption for fewer aerosols.

2) The ~~B_{core}~~Bcore volume fraction increases at smaller mass values (or earlier in cloud's lifetime) and to higher values for increasing aerosol concentration. This effect is complimentary to the previous one, since efficient consumption of super-saturation should result in more latent heat release and positive buoyancy.

3) The core volume fractions of the largest mass clouds increase with increasing aerosol concentration, for all core types.

4) ~~For the dissipating branch clouds~~The mean area of large mass clouds increases significantly with decrease in aerosol concentration.

We also note a general increase in the fraction of clouds that are Wcore or RHcore dominated with increase in aerosol concentration. Meaning adding aerosols shifts a cloud from being mostly margin to being mostly core. The Bcore is an exception since the clean case shows the highest fraction of Bcore dominated clouds and both the clean and polluted cases are more Bcore dominated than the intermediate case. This can be explained by the different mechanisms of buoyancy production (see Sect. 3.2 and 4.2), where the polluted case is positively influenced by updraft buoyancy production and a larger core volume fraction while the frequently precipitating clean case is positively influenced by downdraft buoyancy production. For the dissipating branch clouds, a highly variable pattern of core volume fractions can be seen, especially for the small mass clouds. For all aerosol concentrations, these small cloud fragments can be either core dominated, margin dominated, or equally partitioned. One can assume that these differences can be related to the different mechanisms by which cloud fragments form, either by gradual dissipation of a large cloud and by instantaneous shedding of a large cloud. As for aerosol effects on the dissipating clouds, we see the following:

1) Higher ~~RH_{core}~~RHcore and ~~W_{core}~~Wcore volume fractions for gradually dissipating clouds (by rising cloud base) with increase in aerosol concentration. This is manifested by a slower transition from red to blue colors in Fig. 5. It can be explained by the fact that more aerosols increase the convective intensity and extend the core size, while efficiently losing the margins, yielding a higher core volume fraction out of the total cloud.

2) The likelihood to find dissipating cloud fragments with a ~~B_{core}~~Bcore increases with decrease in aerosol concentration. For the polluted case most of the dissipating clouds lack a ~~B_{core}.~~Bcore. This effect was seen in Fig. 1 and explained in Sect. 3.2, showing that~~ weak~~ downdrafts promote heating and positive buoyancy in low aerosol concentration cases where evaporation efficiency (and hence cooling) is limited. This ~~hypothesis~~effect is checked for the cloud field scale in Sect. 4.2.

As opposed to the single cloud simulations (Sect. 3) where cloud lifetime can be easily defined, in cloud field simulations (especially the cleaner cases) many clouds do not live as individual clouds from formation to dissipation but rather split and merge with other clouds continuously (Heiblum et al., 2016b). Thus, in order to evaluate the lifetime evolution of cores in cloud fields, we focus on the growing branch and use cloud mass [kg] as a proxy for the cloud lifetime during its initial and mature stages. We assume that in the vicinity of the growing branch a larger mass corresponds to a later stage in lifetime.

In Fig. 6 the core mass and volume fractions (using the RH definition) of all growing branch clouds are sorted by mass for the three aerosol concentrations. We note that the higher cloud masses reached by lower aerosol concentration simulation can be explained by cloud field organization effects due to precipitation (i.e. increased merging of clouds) rather than increased cloud condensation (Heiblum et al., 2016b; Seigel, 2014). The clean case starts off with the highest core fractions (both mass and volume) which decrease steadily with increase in mass (or increase in lifetime). For all concentrations, most of the cloud mass is concentrated in the core region. The polluted case shows a slight increase in core mass fractions with increase in mass, while the other two cases show decreases in core mass fractions.

The core volume fractions show lower values than the mass fractions. The clean clouds are margin dominated for most masses, and the polluted clouds are core dominated for all masses. The intermediate case is generally confined to values between the other two cases. Figure 6 can be considered comparable with the lower panels in Fig. 3, but excluding the dissipating part of those time series. The similar findings in both figures indicate the robustness of the aerosol effects on core properties in clouds.

Following the analyses of Sect. 3.1, we next test how aerosol concentration affects the subset properties of one core type within another for all clouds in a field (Fig. 7). We focus only on the typically smaller sized cores (~~B_{core}, RH_{core})~~Bcore, RHcore) within larger sized cores. Out of the three permutations, the ~~RH_{core}~~RHcore inside ~~W_{core}~~Wcore shows the lowest sensitivity to aerosol. All three growing branches (for the different aerosol concentrations) consistently show that the ~~RH_{core}~~RHcore is a subset of ~~W_{core}~~Wcore (i.e.~~ $RH_{core} \subseteq W_{core}$)~~ RHcore ⊂ Wcore) while the dissipation branches show much lower overlap fraction between the two cores.

Generally, for the dissipating clouds, the lower the mass and the higher the COG, the smaller the overlap. The dissipating branches do include a scatter of small cloud for which ~~$RH_{core} \subseteq W_{core}$,~~RHcore ⊂ Wcore, comprised of small cloud segments which shed ~~of~~off the main core regions of larger clouds. These findings slightly differ from those of the single cloud simulations that show ~~$RH_{core} \subseteq W_{core}$~~RHcore ⊂ Wcore for their entire lifetimes while for cloud fields this property breaks downs during dissipation. This difference highlights the importance of cloud interactions (i.e. splitting, merging) and cloud field air flow patterns (i.e. organized advection, updrafts, and downdrafts) in determining the relationships between core types, enabling supersaturation and downdrafts to coincide in small dissipating clouds.

The other two permutations (i.e. ~~B_{core}~~ Bcore inside ~~RH_{core}, W_{core})~~RHcore, Wcore) show significant changes due to aerosol. For the polluted case, ~~$B_{core} \subseteq W_{core}$~~Bcore ⊂ Wcore for nearly all clouds, including clouds at initial stages of dissipation. Similar results are seen for ~~B_{core}~~ Bcore inside ~~RH_{core},~~RHcore, but with slightly lower pixel fractions. The polluted case thus illustrates the case of buoyancy production due to convective ~~processes~~updraft. For the lower aerosol concentrations, two main aerosol effects are seen:

1) The lower the concentration, the lower the chance that ~~B_{core}~~Bcore is a proper subset of the other cores for large growing branch clouds.

2) The lower the concentration, the more prevalent the independent dissipating branch ~~B_{core}~~Bcore that has little to no overlap with the other cores.

For the case of ~~B_{core}~~Bcore within ~~RH_{core},~~ RHcore, the lower concentrations show an almost binary scenario where either ~~$B_{core} \subseteq RH_{core}$~~Bcore ⊂ RHcore or ~~$B_{core} \notin RH_{core}$.~~Bcore ⊄ RHcore. These result bear similarity with the single cloud simulations, where a quick transition (in time) from ~~$B_{core} \subseteq RH_{core}$~~Bcore ⊂ RHcore to ~~$B_{core} \notin RH_{core}$~~Bcore ⊄ RHcore was seen. ~~This~~These results ~~implies~~imply the existence of two different buoyancy production processes (~~as will be shown~~ more in Sect. 4.2), one associated with supersaturation and the other with ~~subsaturation.~~sub-saturation. In contrary, ~~inside, which shows higher values and more fluctuations in~~ pixels fractions of Bcore inside Wcore span the entire range of values (i.e. partial overlaps between the core types), as seen for both single clouds and ~~clouds~~cloud fields during dissipation. This is to be expected due to the a more direct physical link and feedbacks between the ~~B_{core}~~Bcore and ~~W_{core}.~~Wcore.

4.2. Analysis of cloud field buoyancy

In Sect. 3.2 it was seen that for single clouds, positive buoyancy results from two main mechanisms: i) ~~convection~~ convective updrafts - where updrafts promote supersaturation and latent heat release, and thus always positive B_{Qv} and frequently positive B_T ~~and B_{Qv}~~, and ii) ~~adiabatic heating~~dissipative downdrafts – where ~~weak~~sub-saturated cloudy downdrafts promote a positive B_T and neutral B_{Qv}. The latter case is dependent on low evaporation efficiency and hence seen mostly for precipitating stages of low aerosol concentration simulations.

In Fig. 8 we perform a similar test for the cloud field scale. Instead of analyzing pixel by pixel, we check whether each buoyancy core within a cloud is B_T or B_{Qv} dominated. To quantify this we use a normalized buoyancy dominance parameter $\frac{\Sigma pixel_{B_{T}>0}-\Sigma pixel_{B_{Qv}>0}}{\Sigma pixel_{B>0}}$, where a core comprised of only B_T ~~>~~ $\geq$ 0 (B_{Qv} ~~>~~ $\geq$ 0) pixels yields ~~1 (−1~~1 (-1). Hence, we expect negative (positive) values to indicate dominance of ~~convective~~updraft buoyancy (~~adiabatic heating~~downdrafts buoyancy).

Analysis of the buoyancy components in the CvM space (right column, Fig. 8) shows that the large majority of clouds are B_{Qv} dominated. For all concentrations, clouds initiate with all pixels showing B_{Qv} ~~>~~ $\geq$ 0. As clouds develop along the growing branch the ~~B_{core}~~Bcore becomes more abundant with B_T ~~>~~ $\geq$ 0 pixels. This is expected with increasing release of latent heat during cloud growth. During dissipation B_{Qv} again becomes the dominant component for the majority of clouds. The polluted simulation shows an extreme case where all buoyancy cores in the simulation are B_{Qv} dominated, while for the lower concentrations a portion of the dissipating and precipitating clouds are B_T dominated.

Thus, we hypothesize that the polluted simulation only permits buoyancy cores of the ~~convective~~updraft type which intersect with the other ~~cores~~core types (i.e. ~~$B_{core}\in RH_{core},W_{core}$),~~Bcore ∈ RHcore, Wcore), while the lower concentrations also permit buoyancy cores of the ~~adiabatic heating~~downdraft type which do not intersect with the other core types (i.e. ~~$B_{core}\notin RH_{core},W_{core}$). This hypothesis is tested~~Bcore ∉ RHcore, Wcore). We test this by observing the ~~effects~~relation of cloud maximum absolute vertical velocity (left column, Fig. 8) and mean drop size (middle column, Fig. 8) ~~on~~with the relative dominance of the buoyancy terms. Absolute vertical velocity is chosen to represent both updrafts and downdrafts. The data is further separated to independent (~~$B_{core}\notin RH_{core},W_{core}$)~~Bcore ∉ RHcore, Wcore) and dependent (~~$B_{core}\in RH_{core},W_{core}$)~~Bcore ∈ RHcore, Wcore) buoyancy subsets of the data~~.~~, by that separating to buoyant cores within updrafts and downdrafts. Clear aerosol effects are seen on cloud mean drop size and maximal |W~~.~~|. As expected, there is a decrease in drop size with increase in aerosol concentration and increase in maximal velocity.

Regarding cloud field buoyancy, as predicted the independent buoyancy cores are more frequently ~~B_T~~B_T dominated than the dependent buoyancy cores.

The polluted case is populated with dependent cores (white scatter) and shows a classic pre-precipitation convective growth scenario, where relative dominance of the ~~B_T~~B_T term increases linearly with increase in cloud mean drop size. A logarithmic dependence of ~~B_T~~B_T dominance on maximal |W| is seen, which saturates at high maximal |W|. This can be explained by the fact increased convection mainly increases the abundance of pixels with ~~$B_T > 0$~~$B_T > 0$, but without changing the fact that the entire cloud is ~~$B_{Qv} > 0$~~$B_{Qv} > 0$, so that ~~B_T~~B_T is unlikely to become the dominant term.

The lower concentrations show a more complex scenario. These simulations show a superposition of dependent core convective growth behavior (i.e. the scatter pattern seen for the polluted case) and additional populations of both dependent (other white scatter points) and independent (black scatter) cores. ~~The independent cores span all the range of possibilities of B_T and B_{Qv} relative dominances. They tend to have larger cloud mean drop sizes, and near zero maximum W, indicating that they only form at late non-convective stages of cloud development. The independent cores that are $B_T$dominated thus fulfill the characteristics of adiabatic heating process, while the independent cores that are B_{Qv} dominated may originate from larger clouds (shedding mechanism) with high humidity content and are slow to evaporate.~~

The independent cores span all the range of possibilities of B_T and B_{Qv} relative dominances. They tend to have larger cloud mean drop sizes, and near zero maximum |W|, indicating that they only form at late non-convective stages of cloud development. Furthermore, a trend is seen for the subset of scatter that is B_T dominated, where a positive (negative) correlation between mean drop size (maximal |W|) and B_T dominance is seen. This again stresses the importance of drop size on the formation of positive buoyancy within downdrafts, and highlights the fact that B_T should be largest (and most abundant) below the downdraft equilibrium level, when the |W| approaches zero. The independent cores that are B_T dominated thus fulfill the characteristics of downdraft buoyancy production process, while the independent cores that are B_{Qv} dominated may originate from larger clouds (shedding mechanism) with high humidity content, have weak |W|, and are slow to evaporate.

The intermediate simulation shows an additional scatter area of dependent core clouds with increasing of ~~B_T~~B_T relative dominance for lower maximal |W~~,~~|, located between the independent core clouds and the convective growth core clouds. These clouds may represent a gradual transition from~~B_{Qv}~~ B_{Qv} dominance to ~~B_T~~B_T dominance during dissipation which is only possible in the intermediate simulation. This scatter area is absent from the clean and polluted simulation. In the former case due to absence of the gradual dissipation pathway, and in the latter case due to efficient evaporation eliminating ~~B_{core} during dissipation.~~Bcore during dissipation. We note that the intermediate case shows a slightly higher percentage of clouds that are B_T dominated (see legends in Fig. 8) than the clean case. This can be due to stronger convection in this simulation (i.e. increased |W| range), which favors increased mixing with the dry environment (see Fig. 9) and the formation of unsaturated strong downdrafts that descend below the level of neutral buoyancy.

4.3. Aerosol effects on cloud relative humidity

From Fig. 3 it was learned that a large part of the differences in single cloud characteristics (such as mass, volume, and the partition of these to core and margin regions) due to aerosols can be attributed to differences in vapor diffusion efficiencies. In Fig. 9 we check how these aerosol effects are manifested in the cloud field scale (using the CvM space) by observing the mean relative humidity (RH) in the cloud core and margin of all clouds~~. The~~, where the core (margin) mean RH can be taken as a proxy for condensation ~~efficiency, the margin mean RH as a proxy for~~ (evaporation) efficiency. To gain additional intuition regarding the distribution of RH values within the clouds, vertical cross-sections (parallel to the prevailing wind direction) of the most massive clouds from each simulation are shown.

The vertical cross-sections demonstrate the large differences in the massive clouds for each of the simulations. In addition to the increase in precipitation production, lower aerosol concentrations yield much larger horizontal extents of clouds. The clean, intermediate, and polluted most massive clouds have a maximum radius of ~ 3, ~ 1, and ~ 0.5 km, respectively. It is clear from the cross-section that the clean cloud is actually composed of two large clouds which merge together. For the clean case, the highest RH values are reached slightly below the cloud top. The edges of the clouds show sub-saturation conditions, with the lowest RH values observed below the LCL (precipitation regions) and at the upper interface of the cloud with the environments.

The intermediate case cloud shows lower maximal and minimal RH values and an increased dominance of the margin region. This cloud penetrates the inversion layer and entrains dry air into the cloud. In addition, the cloud produces significant precipitation which initiates downdrafts of dry entrained air through the cloud center. It can be seen that the increased vertical development of the intermediate case cloud in comparison with the clean case increases the mixing with the environment. Thus, the dynamic effect of increased mixing and reduction in cloud RH overcomes the microphysical effect of increased evaporation and increase in cloud RH. The polluted case cloud on the other hand shows a homogeneous RH pattern, with most of the cloud showing around 100% RH and only a thin layer at the cloud edges (mainly at the upper regions) shows lower RH values. The polluted cloud penetrates the inversion layer as well, but this case lacks precipitation and the microphysical effect of evaporation overcomes the dynamical effect of mixing.

Keeping in mind the insights obtained from comparisons of individual cloud, we move on to compare the RH characteristics of all clouds within the field. Looking first at core mean RH, a robust decrease is seen with increase in aerosol concentration. This decrease is seen for all cloud types and locations within the CvM space. The polluted case displays the most homogeneous pattern with all clouds showing core mean RH values around 100%, indicating efficient consumption of the supersaturation. The intermediate case displays a slightly less homogeneous pattern with values ranging from 100% to 101%, the higher values occurring along the growing cloud branch, especially for the largest clouds. The clean case shows the largest variance in core mean RH, ranging from 100% for some cloud fragments that soon start to dissipate, to 103% in the cores of the large cloud entities. In addition to the low efficiency in consuming supersaturation, the high RH values in clean large clouds are due to the "protection" by large margin regions surrounding the core region.

The CvM patterns of mean margin RH show significant differences between the polluted case and the other two. The mean margin RH values of the polluted case are only marginally lower than 100%, since sub-saturated conditions within the cloud are quickly adjusted by efficient evaporation. Only the largest clouds in the polluted case permit lower mean margin RH values (~ 95%) due to the entrainment of very dry environmental pixels near the cloud tops (as seen in the vertical cross-section as well). The intermediate and clean cases show similar patterns. The smaller mass clouds (both growing and dissipating) show values above 95%, while the larger mass clouds show values as low as 85%. The larger clouds are most likely to reach low RH areas near the inversion base and below the LCL (i.e. sub-cloudy layer) and entrain dry air and by that reduce the cloud margin RH.

As seen in the vertical cross-section examples, the largest clouds in the intermediate case have even lower margin RH values than for the clean case. This can be explained by the increased development of the large intermediate clouds to heights with lower RH and by more intense downdrafts for these large clouds. The lowest RH values in the domain are seen for the precipitating fragments (i.e. located below the adiabat). These fragments typically contain low concentrations of large drop sizes (precipitation drops) which are slow to evaporate and capable of surviving in low RH conditions within the sub-cloudy layer.

Summary

In this work we explored how the aerosol effects on warm convective clouds are reflected in their partition to core and margin regions. Following part I of this work (PTI), we evaluated three types of core definitions: positive buoyancy (~~B_{core}),~~Bcore), super-saturation (~~RH_{core}),~~RHcore), and positive vertical velocity (~~W_{core}).~~Wcore). Both single cloud and cloud field models have been used. ~~The former distills the dominant in-cloud processes affected by aerosols while the latter also takes into consideration the multiple temporal cloud evolution pathways and the additional effects of cloud field organization and interactions between clouds.~~

For all aerosol concentrations~~,~~ (clean, intermediate, and polluted) it is shown that the self-contained property of different core types (i.e. ~~$B_{core} \subseteq RH_{core} \subseteq W_{core}$~~Bcore $\subset$ RHcore $\subset$ Wcore) is maintained for clouds during their growing and mature stages. This is especially robust for the ~~$RH_{core} \subseteq W_{core}$~~RHcore $\subset$ Wcore subset. The

~~W_{core}~~Wcore and ~~RH_{core}~~RHcore volume fractions decrease monotonically during cloud growth, while ~~B_{core}~~Bcore initially increases and then decreases after convection ceases. During growth, the ~~RH_{core} (B_{core})~~RHcore (Bcore) volume fractions are largest for clean (polluted) clouds. This is due to low (high) diffusion efficiencies, respectively, where efficient condensation promotes ~~B_{core}~~Bcore at the expense of ~~theRH_{core}.~~the RHcore.

During dissipation stages cores frequently cease to be subsets of one another and may either increase or decrease in their volume fractions. In cloud fields we also observe small cloud fragments which shed off larger cloud entities. This shedding increases for the lower concentration simulation which produce long-lived large cloud entities~~.~~ due to cloud merging. These fragments show large variance in volume fraction (for all core types) magnitudes without any consistent behavior. This is due to the fact that they shed off various locations of the cloud. The polluted, non-precipitating cases, are unique in that can one expect the ~~B_{core}~~Bcore to decrease monotonically and remain the smallest and a proper subset of the other cores.

For low aerosol ~~concentration, clouds which are capable of producing precipitation~~concentrations, a ~~B_{core}~~Bcore may form during dissipation and exist independently of the other core types. These cores are typically located at the periphery of large clouds, or throughout small precipitation or dissipating cloud fragments. The increase in ~~B_{core}~~Bcore during dissipation typically coincides with large drop sizes and precipitation production. The fluctuations in ~~B_{core}~~Bcore for low concentrations may also create a subsequent ~~W_{core},~~Wcore, but not of sufficient strength to also create a ~~RH_{core}.~~RHcore. Hence, the ~~RH_{core}~~RHcore can be considered the most “well-behaved” and indicative of cloud lifetime, generally monotonically decreasing in volume fraction irrespective of aerosol concentration.

We show that the ~~B_{core}~~Bcore in the warm convective cases considered here may form by two main processes:

1. ~~Convection~~Convective updrafts: adiabatic cooling within updrafts promotes supersaturation, condensation, and release of latent heat. These cores are characterized by both positive temperature ($B_T > 0$) and humidity ($B_{Qv} > 0$) buoyancy terms.

~~2. Adiabatic heating: weak~~Dissipative downdrafts~~ during dissipation or precipitation transport higher potential temperatures from above.~~

2. ~~The convective case~~: sub-saturated cloudy downdrafts follow a lapse rate which is ~~seen for all aerosol concentrations, and is~~unstable relative to the environmental one. These downdrafts undershoot the equilibrium level and become positively buoyant. These cores are characterized by ~~a dependent B_{core} (i.e. $B_{core} \in RH_{core}, W_{core}$). During convection B_{core} pixels have a positive humidity term (B_{Qv}), with an increasing abundance of a~~ positive temperature ~~term (B_T) pixels with increase in cloud maximum vertical velocities. During dissipation this type of B_{core} shrinks rapidly due to negative B_T. The adiabatic heating case~~ ($B_T > 0$) but neutral humidity ($B_{Qv} \sim 0$) buoyancy terms.

The updraft buoyancy type is seen for all aerosol concentrations, while the dissipation buoyancy type is only seen for lower aerosol concentrations~~, and is characterized by independent B_{core} (i.e. $B_{core} \notin RH_{core}, W_{core}$). In this case B_T is the dominant term in the cloud. The clouds with independent B_{core} experience near neutral vertical velocities for all pixels, and typically show larger cloud mean drop sizes than for the dependent type ones.~~

~~The~~. The fact that the ~~adiabatic heating B_{core}~~downdraft Bcore is absent from polluted clouds highlights the importance of ~~mean~~ drop size and its effect on evaporation rate. The high (low) diffusion (collision coalescence) efficiencies in polluted clouds maintain a small mean drop size and ~~efficient~~enable rapid evaporation during entrainment~~. In PTI we saw that evaporation always has~~, causing a ~~strong~~ negative effect on buoyancy. ~~In the polluted case the convective B_{core} disappear rapidly during dissipation and cannot form in small cloud fragments even if they experience weak downdrafts. The importance of drop size is illustrated by the fact that even for~~For lower concentrations, clouds with ~~independent B_{core}~~a downdraft Bcore only exist during late mature, dissipation, and precipitating stages after drop size has grown considerably. The larger mean drop sizes reduce evaporation rates and the cloudy downdrafts may thus descend nearly dry adiabatically and become positively buoyant.

Focusing on cores using the RH definition, a cloud's mass (volume) is dependent primarily on the processes in its core (margin). The core increases cloud mass by condensation while the margin increases the cloud's volume by mixing with the environment, or dilution. The magnitude of the effects in each region of the cloud is strongly dependent on the aerosol concentration. ~~Increasing the aerosol concentration increases the vapor diffusion rate, minimizing both the super-saturation and sub-saturation (absolute) values in the cloud. Thus, polluted clouds are efficient in accumulating water mass but also in losing it. This competition between the core mass gain and margin mass loss regions is what brings about the concept of an optimal aerosol concentration (Dagan et al., 2015b), and explains why more polluted clouds are not necessarily more massive.~~

Polluted clouds are core dominated both in terms of mass and volume, since they can hardly maintain their margins. Clean clouds are also core dominated in terms of mass, but to a lesser degree. ~~However, expect for the initial time of cloud formation where the entire cloud is super-saturated, clean~~Clean clouds tend to be margin dominated in terms of volume for most their lifetimes. Thus, despite weaker convection in the clean clouds, their large, slow evaporating margins enable their cores (and the entire cloud) to exist for longer time spans by applying a large "protecting shield" around the core.

The different diffusion efficiencies are demonstrated by observing the relative humidity (RH) values in clouds. Cleaner clouds show larger variance in RH values. During their growing stages large super-saturation in the core and sub-saturation in the margin can be seen. During their dissipation stages clouds may exist for minutes without any cloud core, with the entire cloud at sub-saturation. Polluted clouds show the opposite, with RH values nearing 100% throughout the cloud, at all stages. Hence, above a certain aerosol concentration, the saturation adjustment approximation (i.e. instant condensation of all super-saturation) can be considered valid. However, the transition from clean to polluted is not always linear. For example, for the largest clouds in the intermediate case have lower margin RH value than both the clean and polluted cases. This is due to the fact that the intermediate case manages to develop taller (than the clean case) clouds with stronger updrafts and downdrafts which entrain drier air from above the inversion layer base, but at the same time is less efficient in evaporating (than the polluted case) water and adjusting the RH to 100%.

~~Finally, we note that the cloud organization also changes with aerosol concentration, and thus serves as an additional factor affecting the cloud partition to core and margin.~~

~~Decreasing the aerosol concentration increases the precipitation yield, which alters the sub-cloudy layer organization and promotes merging between different clouds (Heiblum et al., 2016b; Seifert and Heus, 2013; Seigel, 2014). These effects are minimal in the polluted cases. Hence, to a first approximation polluted cloud fields can be considered as a superposition of many single clouds while clean cloud fields behave very differently than a collection of single clean clouds. The continuous merging between clean clouds creates large cloud entities that evolve along relatively long times. These large precipitating entities also frequently shed small cloud fragments into the upper cloudy layer. This effect, combined with the low vapor diffusion, explains why clean clouds tend to be even more margin dominated (in terms of volume) during growth, while showing larger core fractions (especially B_{core}) during dissipation.~~

Author Contributions

RH ran cloud field simulations and conducted the analyses, and wrote the final draft of paper. LP participated in writing the first draft, and performed single cloud simulations and relevant analyses. OA, GD, and IK participated in paper editing and discussions.

Acknowledgements

The research leading to these results was supported by the Ministry of Science & Technology, Israel (grant no. 3-14444).

References

Albrecht, B. A.: Aerosols, cloud microphysics, and fractional cloudiness., Science, 245(4923), 1227–1230, doi:10.1126/science.245.4923.1227, 1989.

Altaratz, O., Koren, I., Reisin, T., Kostinski, A., Feingold, G., Levin, Z. and Yin, Y.: Aerosols' influence on the interplay between condensation, evaporation and rain in warm cumulus cloud, Atmos. Chem. Phys., 8(1), 15–24, doi:10.5194/acp-8-15-2008, 2008.

Altaratz, O., Koren, I., Remer, L. A. and Hirsch, E.: Review: Cloud invigoration by aerosols—Coupling between microphysics and dynamics, Atmos. Res., 140-141, 38–60, doi:10.1016/j.atmosres.2014.01.009, 2014.

Andreae, M. O., Rosenfeld, D., Artaxo, P., Costa, A. A., Frank, G. P., Longo, K. M. and Silva-Dias, M. A. F.: Smoking rain clouds over the Amazon., Science, 303(5662), 1337–1342, doi:10.1126/science.1092779, 2004.

Betts, A. K.: Saturation point analysis of moist convective overturning, J. Atmos. Sci., 39(7), 1484–1505, doi:10.1175/1520-0469(1982)039<1484:SPAOMC>2.0.CO;2, 1982.

Betts, A. K. and Silva Dias, M. F.: Unsaturated downdraft thermodynamics in cumulonimbus, J. Atmos. Sci., 36(6), 1061–1071, doi:10.1175/1520-0469(1979)036<1061:UDTIC>2.0.CO;2, 1979.

Carrió, G. G. and Cotton, W. R.: On the buffering of CCN impacts on wintertime orographic clouds: An idealized examination, Atmos. Res., 137, 136–144, doi:10.1016/j.atmosres.2013.09.011, 2014.

Dagan, G., Koren, I. and Altaratz, O.: Aerosol effects on the timing of warm rain processes, Geophys. Res. Lett., 42(11), 4590–4598, doi:10.1002/2015GL063839, 2015a.

Dagan, G., Koren, I. and Altaratz, O.: Competition between core and periphery-based processes in warm convective clouds – from invigoration to suppression, Atmos. Chem. Phys., 15(5), 2749–2760, doi:10.5194/acp-15-2749-2015, 2015b.

Dagan, G., Koren, I., Altaratz, O. and Heiblum, R. H.: Aerosol effect on the evolution of the thermodynamic properties of warm convective cloud fields., Sci. Rep., 6, 38769, doi:10.1038/srep38769, 2016.

Dagan, G., Koren, I., Altaratz, O. and Heiblum, R. H.: Time-dependent, non-monotonic response of warm convective cloud fields to changes in aerosol loading, Atmos. Chem. Phys., 17(12), 7435–7444, doi:10.5194/acp-17-7435-2017, 2017.

Dey, S., Di Girolamo, L., Zhao, G., Jones, A. L. and McFarquhar, G. M.: Satellite-observed relationships between aerosol and trade-wind cumulus cloud properties over the Indian Ocean, Geophys. Res. Lett., 38(1), doi:10.1029/2010GL045588, 2011.

Glassmeier, F. and Lohmann, U.: Precipitation Susceptibility and Aerosol Buffering of Warm- and Mixed-Phase Orographic Clouds in Idealized Simulations, J. Atmos. Sci., 75(4), 1173–1194, doi:10.1175/JAS-D-17-0254.1, 2018.

Grant, L. D. and van den Heever, S. C.: Cold pool and precipitation responses to aerosol loading: modulation by dry layers, J. Atmos. Sci., 72(4), 1398–1408, doi:10.1175/JAS-D-14-0260.1, 2015.

Heiblum, R. H., Altaratz, O., Koren, I., Feingold, G., Kostinski, A. B., Khain, A. P., Ovchinnikov, M., Fredj, E., Dagan, G., Pinto, L., Yaish, R. and Chen, Q.: Characterization of cumulus cloud fields using trajectories in the center of gravity versus water mass phase space: 1. Cloud tracking and phase space description, J. Geophys. Res. Atmos., 121(11), 6336–6355, doi:10.1002/2015JD024186, 2016a.

Heiblum, R. H., Altaratz, O., Koren, I., Feingold, G., Kostinski, A. B., Khain, A. P., Ovchinnikov, M., Fredj, E., Dagan, G., Pinto, L., Yaish, R. and Chen, Q.:

Characterization of cumulus cloud fields using trajectories in the center of gravity versus water mass phase space: 2. Aerosol effects on warm convective clouds, J. Geophys. Res. Atmos., 121(11), 6356–6373, doi:10.1002/2015JD024193, 2016b.

Hudson, J. G. and Mishra, S.: Relationships between CCN and cloud microphysics variations in clean maritime air, Geophys. Res. Lett., 34(16), doi:10.1029/2007GL030044, 2007.

Hudson, J. G. and Yum, S. S.: Maritime–continental drizzle contrasts in small cumuli, J. Atmos. Sci., 58(8), 915–926, doi:10.1175/1520-0469(2001)058<0915:MCDCIS>2.0.CO;2, 2001.

Igau, R. C., LeMone, M. A. and Wei, D.: Updraft and downdraft cores in TOGA COARE: why so many buoyant downdraft cores?, J. Atmos. Sci., 56(13), 2232–2245, doi:10.1175/1520-0469(1999)056<2232:UADCIT>2.0.CO;2, 1999.

IPCC: Climate Change 2013: The Physical Science Basis. Working Group I Contribution to the Fifth Assessment Report of the IPCC, Cambridge Univ. Press, New York., 2013.

Jaenicke, R.: 9.3.1 Physical properties, in Physical and chemical properties of the air, edited by G. Fischer, pp. 405–420, Springer-Verlag, Berlin/Heidelberg., 1988.

Jiang, H. and Feingold, G.: Effect of aerosol on warm convective clouds: Aerosol-cloud-surface flux feedbacks in a new coupled large eddy model, J. Geophys. Res., 111(D1), doi:10.1029/2005JD006138, 2006.

Jiang, H., Feingold, G. and Koren, I.: Effect of aerosol on trade cumulus cloud morphology, J. Geophys. Res., 114(D11), doi:10.1029/2009JD011750, 2009.

Jiang, H., Xue, H., Teller, A., Feingold, G. and Levin, Z.: Aerosol effects on the lifetime of shallow cumulus, Geophys. Res. Lett., 33(14), doi:10.1029/2006GL026024, 2006.

Kaufman, Y. J., Koren, I., Remer, L. A., Rosenfeld, D. and Rudich, Y.: The effect of smoke, dust, and pollution aerosol on shallow cloud development over the Atlantic Ocean., Proc. Natl. Acad. Sci. USA, 102(32), 11207–11212, doi:10.1073/pnas.0505191102, 2005.

Khain, A. P., BenMoshe, N. and Pokrovsky, A.: Factors Determining the Impact of Aerosols on Surface Precipitation from Clouds: An Attempt at Classification, J. Atmos. Sci., 65(6), 1721–1748, doi:10.1175/2007JAS2515.1, 2008.

Khain, A., Pokrovsky, A., Pinsky, M., Seifert, A. and Phillips, V.: Simulation of Effects of Atmospheric Aerosols on Deep Turbulent Convective Clouds Using a Spectral Microphysics Mixed-Phase Cumulus Cloud Model. Part I: Model Description and Possible Applications, J. Atmos. Sci., 61(24), 2963–2982, doi:10.1175/JAS-3350.1, 2004.

Khain, A., Rosenfeld, D. and Pokrovsky, A.: Aerosol impact on the dynamics and microphysics of deep convective clouds, Q.J Royal Met. Soc., 131(611), 2639–2663, doi:10.1256/qj.04.62, 2005.

Khairoutdinov, M. F. and Randall, D. A.: Cloud resolving modeling of the ARM summer 1997 IOP: model formulation, results, uncertainties, and sensitivities, J. Atmos. Sci., 60(4), 607–625, doi:10.1175/1520-0469(2003)060<0607:CRMOTA>2.0.CO;2, 2003.

Knupp, K. R. and Cotton, W. R.: Convective cloud downdraft structure: An interpretive survey, Rev. Geophys., 23(2), 183, doi:10.1029/RG023i002p00183, 1985.

Kogan, Y. L. and Martin, W. J.: Parameterization of bulk condensation in numerical cloud models, J. Atmos. Sci., 51(12), 1728–1739, doi:10.1175/1520-0469(1994)051<1728:POBCIN>2.0.CO;2, 1994.

Köhler, H.: The nucleus in and the growth of hygroscopic droplets, Transactions of the Faraday Society, 32, 1152–1161, 1936.

Koren, I., Altaratz, O. and Dagan, G.: Aerosol effect on the mobility of cloud droplets, Environmental Research Letters, 10(10), 104011, doi:10.1088/1748-9326/10/10/104011, 2015.

Koren, I., Dagan, G. and Altaratz, O.: From aerosol-limited to invigoration of warm convective clouds., Science, 344(6188), 1143–1146, doi:10.1126/science.1252595, 2014.

L'Ecuyer, T. S., Berg, W., Haynes, J., Lebsock, M. and Takemura, T.: Global observations of aerosol impacts on precipitation occurrence in warm maritime clouds, J. Geophys. Res., 114(D9), doi:10.1029/2008JD011273, 2009.

Li, Z., Niu, F., Fan, J., Liu, Y., Rosenfeld, D. and Ding, Y.: Long-term impacts of aerosols on the vertical development of clouds and precipitation, Nat. Geosci., 4(12), 888–894, doi:10.1038/ngeo1313, 2011.

Mason, B. J. and Chien, C. W.: Cloud-droplet growth by condensation in cumulus, Quarterly Journal of the Royal Meteorological Society, 88(376), 136–142, 1962.

Mordy, W.: Computations of the growth by condensation of a population of cloud droplets, Tellus, 11(1), 16–44, doi:10.1111/j.2153-3490.1959.tb00003.x, 1959.

Paluch, I. R. and Breed, D. W.: A Continental Storm with a Steady, Adiabatic Updraft and High Concentrations of Small Ice Particles: 6 July 1976 Case Study, J. Atmos. Sci., 41(6), 1008–1024, doi:10.1175/1520-0469(1984)041<1008:ACSWAS>2.0.CO;2, 1984.

Pinsky, M., Mazin, I. P., Korolev, A. and Khain, A.: Supersaturation and diffusional droplet growth in liquid clouds, J. Atmos. Sci., 70(9), 2778–2793, doi:10.1175/JAS-D-12-077.1, 2013.

Reisin, T., Levin, Z. and Tzivion, S.: Rain Production in Convective Clouds As Simulated in an Axisymmetric Model with Detailed Microphysics. Part I: Description of the Model, J. Atmos. Sci., 53(3), 497–519, doi:10.1175/1520-0469(1996)053<0497:RPICCA>2.0.CO;2, 1996.

Reutter, P., Su, H., Trentmann, J., Simmel, M., Rose, D., Gunthe, S. S., Wernli, H., Andreae, M. O. and Pöschl, U.: Aerosol- and updraft-limited regimes of cloud droplet formation: influence of particle number, size and hygroscopicity on the activation of cloud condensation nuclei (CCN), Atmos. Chem. Phys., 9(18), 7067–7080, doi:10.5194/acp-9-7067-2009, 2009.

Saleeby, S. M., Herbener, S. R., van den Heever, S. C. and L'Ecuyer, T.: Impacts of cloud droplet–nucleating aerosols on shallow tropical convection, J. Atmos. Sci., 72(4), 1369–1385, doi:10.1175/JAS-D-14-0153.1, 2015.

Savane, O., Vant-Hull, B., Mahani, S. and Khanbilvardi, R.: Effects of aerosol on cloud liquid water path: statistical method a potential source for divergence in past observation based correlative studies, Atmosphere, 6(3), 273–298, doi:10.3390/atmos6030273, 2015.

Seifert, A. and Heus, T.: Large-eddy simulation of organized precipitating trade wind cumulus clouds, Atmos. Chem. Phys., 13(11), 5631–5645, doi:10.5194/acp-13-5631-2013, 2013.

Seifert, A., Heus, T., Pincus, R. and Stevens, B.: Large-eddy simulation of the transient and near-equilibrium behavior of precipitating shallow convection, J. Adv. Model. Earth Syst., 7(4), 1918–1937, doi:10.1002/2015MS000489, 2015.

Seigel, R. B.: Shallow Cumulus Mixing and Subcloud-Layer Responses to Variations in Aerosol Loading, J. Atmos. Sci., 71(7), 2581–2603, doi:10.1175/JAS-D-13-0352.1, 2014.

Seiki, T. and Nakajima, T.: Aerosol effects of the condensation process on a convective cloud simulation, J. Atmos. Sci., 71(2), 833–853, doi:10.1175/JAS-D-12-0195.1, 2014.

Sheffield, A. M., Saleeby, S. M. and van den Heever, S. C.: Aerosol-induced mechanisms for cumulus congestus growth, J. Geophys. Res. Atmos., 120(17), 8941–8952, doi:10.1002/2015JD023743, 2015.

Siebesma, A. P., Bretherton, C. S., Brown, A., Chlond, A., Cuxart, J., Duynkerke, P. G., Jiang, H., Khairoutdinov, M., Lewellen, D., Moeng, C.-H., Sanchez, E., Stevens, B. and Stevens, D. E.: A large eddy simulation intercomparison study of shallow cumulus convection, J. Atmos. Sci., 60(10), 1201–1219, doi:10.1175/1520-0469(2003)60<1201:ALESIS>2.0.CO;2, 2003.

Small, J. D., Chuang, P. Y., Feingold, G. and Jiang, H.: Can aerosol decrease cloud lifetime?, Geophys. Res. Lett., 36(16), doi:10.1029/2009GL038888, 2009.

Sorooshian, A., Feingold, G., Lebsock, M. D., Jiang, H. and Stephens, G. L.: On the precipitation susceptibility of clouds to aerosol perturbations, Geophys. Res. Lett., 36(13), doi:10.1029/2009GL038993, 2009.

Squires, P.: The microstructure and colloidal stability of warm clouds, Tellus, 10(2), 256–261, doi:10.1111/j.2153-3490.1958.tb02011.x, 1958.

Stevens, B.: On the growth of layers of nonprecipitating cumulus convection, J. Atmos. Sci., 64(8), 2916–2931, doi:10.1175/JAS3983.1, 2007.

Stevens, B. and Feingold, G.: Untangling aerosol effects on clouds and precipitation in a buffered system., Nature, 461(7264), 607–613, doi:10.1038/nature08281, 2009.

Storer, R. L. and van den Heever, S. C.: Microphysical processes evident in aerosol forcing of tropical deep convective clouds, J. Atmos. Sci., 70(2), 430–446, doi:10.1175/JAS-D-12-076.1, 2013.

Twomey, S.: The influence of pollution on the shortwave albedo of clouds, J. Atmos. Sci., 34(7), 1149–1152, doi:10.1175/1520-0469(1977)034<1149:TIOPOT>2.0.CO;2, 1977.

Tzivion, S., Feingold, G. and Levin, Z.: An efficient numerical solution to the stochastic collection equation, J. Atmos. Sci., 44(21), 3139–3149, doi:10.1175/1520-0469(1987)044<3139:AENSTT>2.0.CO;2, 1987.

Wang, C.: A modeling study of the response of tropical deep convection to the increase of cloud condensation nuclei concentration: 1. Dynamics and microphysics, J. Geophys. Res., 110(D21), doi:10.1029/2004JD005720, 2005.

Warner, J.: A Reduction in Rainfall Associated with Smoke from Sugar-Cane Fires—An Inadvertent Weather Modification?, J. Appl. Meteor., 7(2), 247–251, doi:10.1175/1520-0450(1968)007<0247:ARIRAW>2.0.CO;2, 1968.

Wei, D., Blyth, A. M. and Raymond, D. J.: Buoyancy of convective clouds in TOGA COARE, J. Atmos. Sci., 55(22), 3381–3391, doi:10.1175/1520-0469(1998)055<3381:BOCCIT>2.0.CO;2, 1998.

Xu, K.-M. and Randall, D. A.: Updraft and downdraft statistics of simulated tropical and midlatitude cumulus convection, J. Atmos. Sci., 58(13), 1630–1649, doi:10.1175/1520-0469(2001)058<1630:UADSOS>2.0.CO;2, 2001.

Xue, H. and Feingold, G.: Large-Eddy Simulations of Trade Wind Cumuli: Investigation of Aerosol Indirect Effects, J. Atmos. Sci., 63(6), 1605–1622, doi:10.1175/JAS3706.1, 2006.

Xue, H., Feingold, G. and Stevens, B.: Aerosol effects on clouds, precipitation, and the organization of shallow cumulus convection, J. Atmos. Sci., 65(2), 392–406, doi:10.1175/2007JAS2428.1, 2008.

Yuan, T., Remer, L. A. and Yu, H.: Microphysical, macrophysical and radiative signatures of volcanic aerosols in trade wind cumulus observed by the A-Train, Atmos. Chem. Phys., 11(14), 7119–7132, doi:10.5194/acp-11-7119-2011, 2011.

Zhao, M. and Austin, P. H.: Life cycle of numerically simulated shallow cumulus clouds. part I: transport, J. Atmos. Sci., 62(5), 1269–1290, doi:10.1175/JAS3414.1, 2005a.

Zhao, M. and Austin, P. H.: Life cycle of numerically simulated shallow cumulus clouds. part II: mixing dynamics, J. Atmos. Sci., 62(5), 1291–1310, doi:10.1175/JAS3415.1, 2005b.

Figures

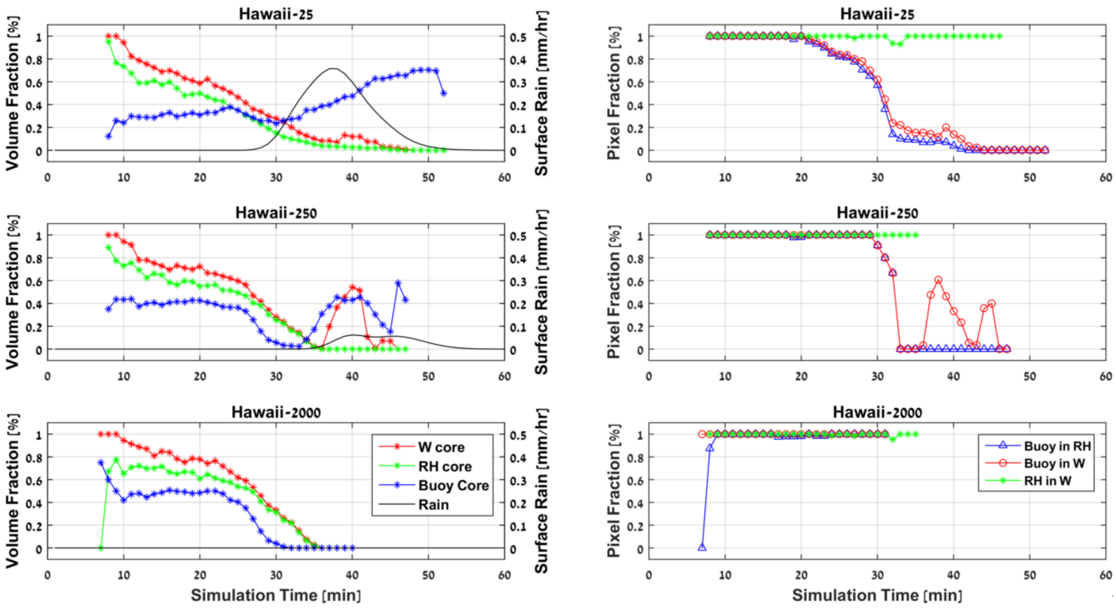

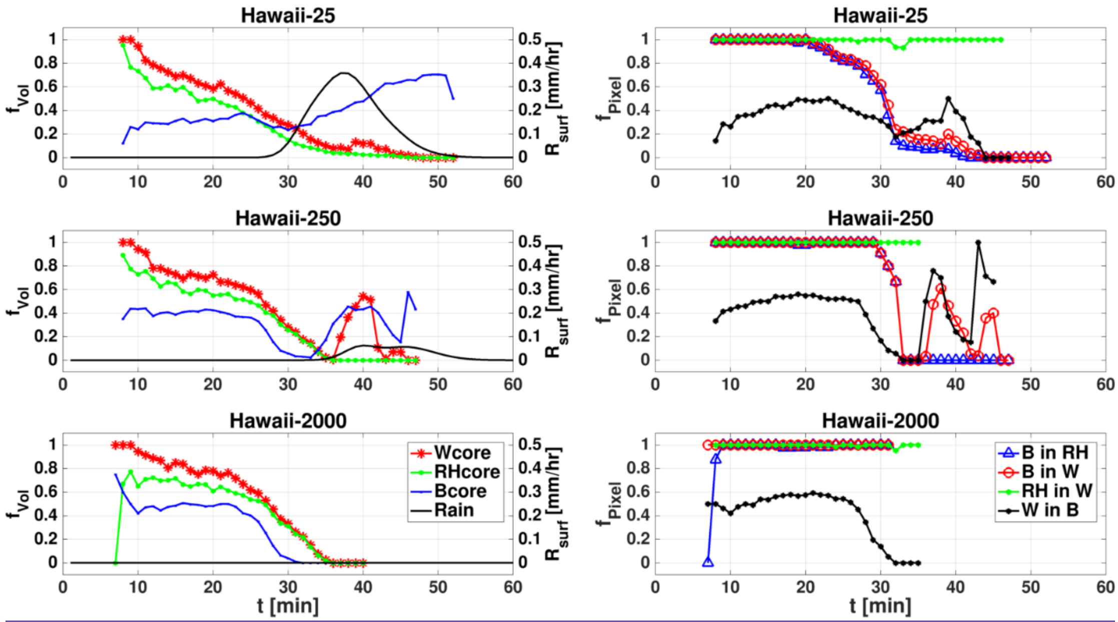

Figure 1. Left: Time series of core volume fractions ~~([%], LHS~~(f_{vol} [%], left axis) and surface rain-rate ~~([~~(R_{surf} [mm hr^{-1}], ~~RHS~~right axis) for the clean (top panel), intermediate (middle panel), and polluted (bottom panel) single cloud simulations. Right: Time series of ~~core~~ pixel fractions (f_{pixel} [%]) of one core type within ~~other core types [%],~~ another, for the respective simulation types. Core volume and pixel fractions are indicated by different line colors (see legends).

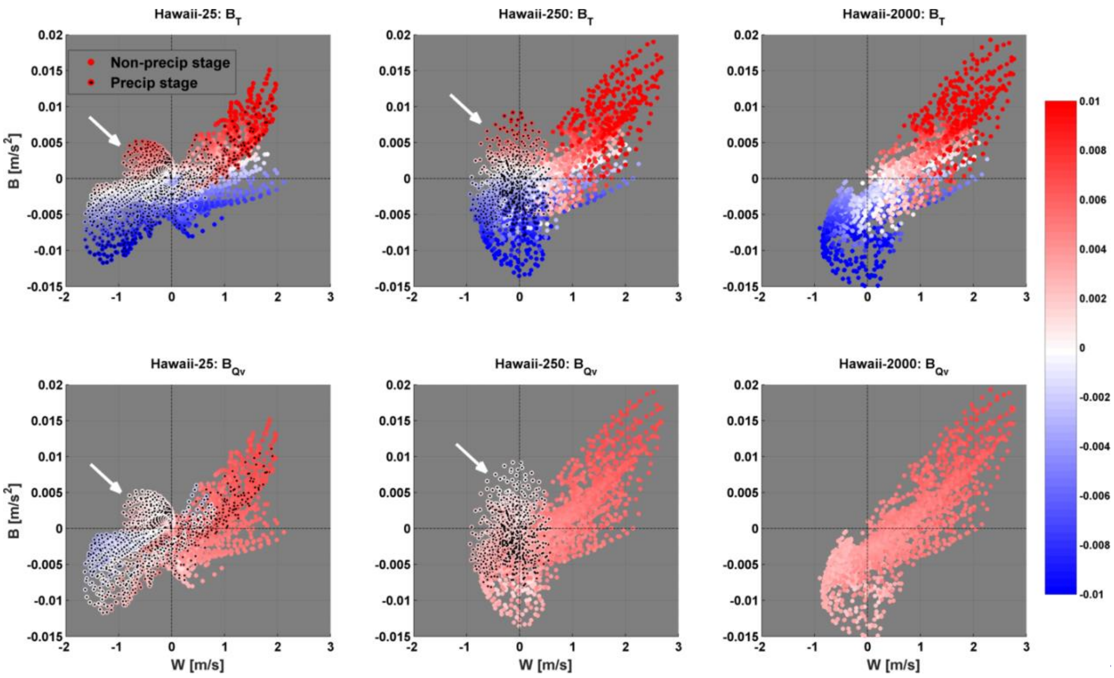

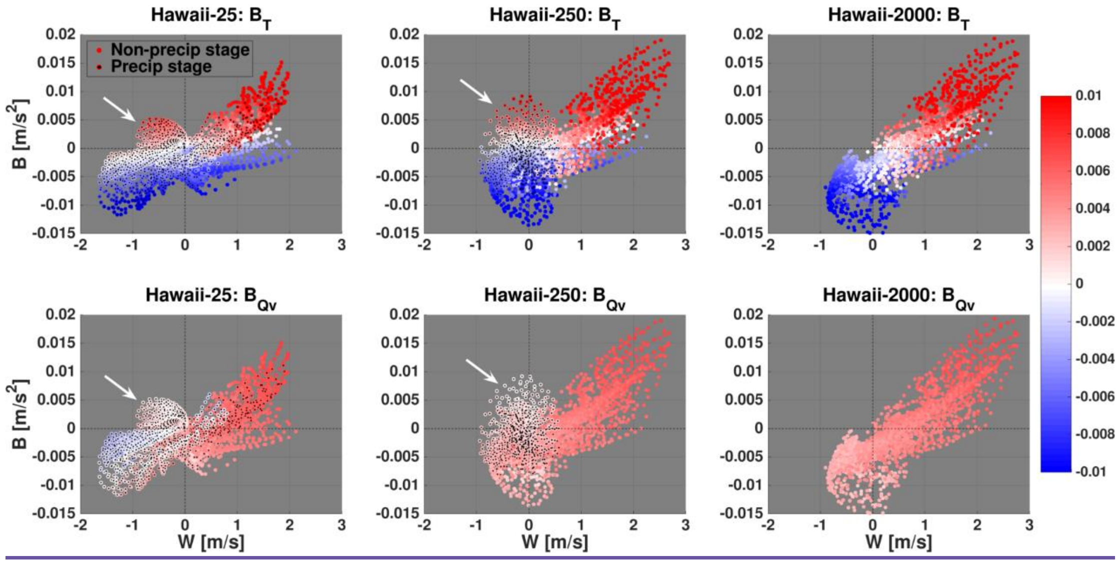

Figure 2. Scatter plots of pixel total buoyancy [m s^{-2}] vs. pixel vertical velocity [m s^{-1}], for the clean (left), intermediate (middle), and polluted (right) simulations. Data includes all cloudy pixels during all time steps. Colors represent magnitude of buoyancy temperature term (B_T, upper row) and humidity term (B_{Qv}, lower row), where red (blue) shades indicate positive (negative) values. Markers with black dots superimposed represent temporal stages with non-zero surface precipitation. White arrows indicate outlier scatter of pixels with positive buoyancy and negative vertical velocity.

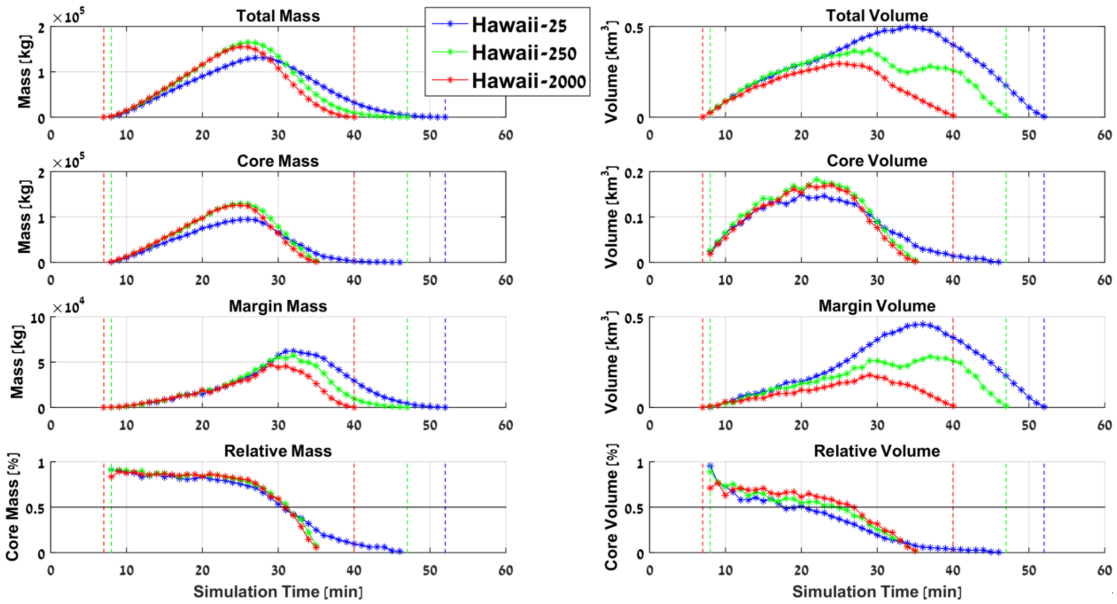

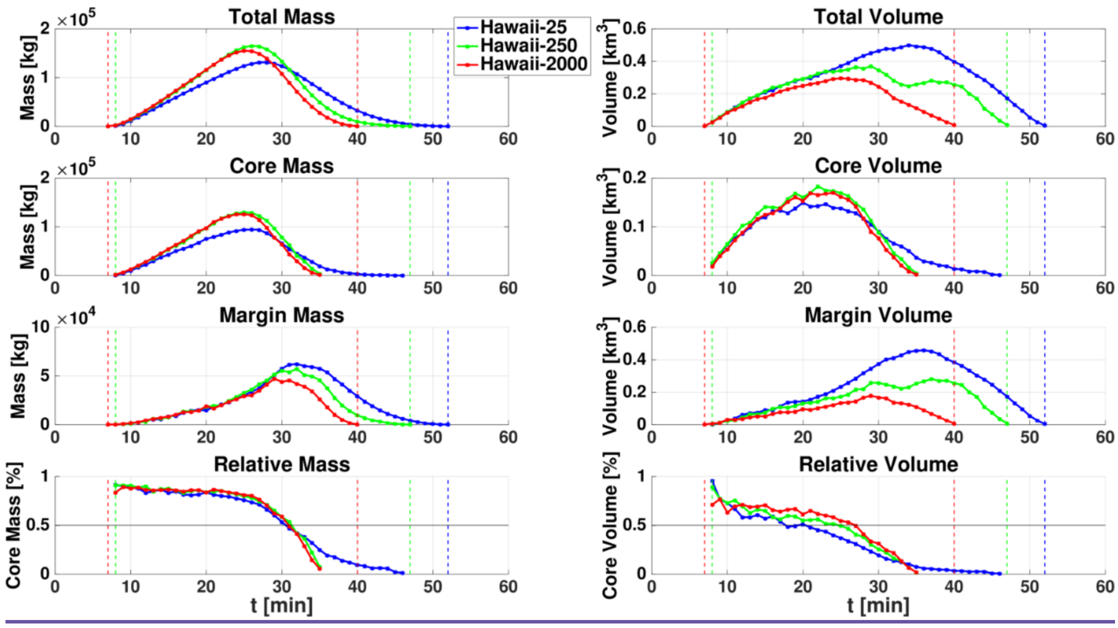

Figure 3. Time series of cloud mass ([kg], left column) and cloud volume ([km^3], right column) for the different aerosol concentrations simulations (see legend). The total, core, margin, and relative fraction values are shown for each parameter, as indicated by panel titles. The core here is defined according to RH>100% definition.

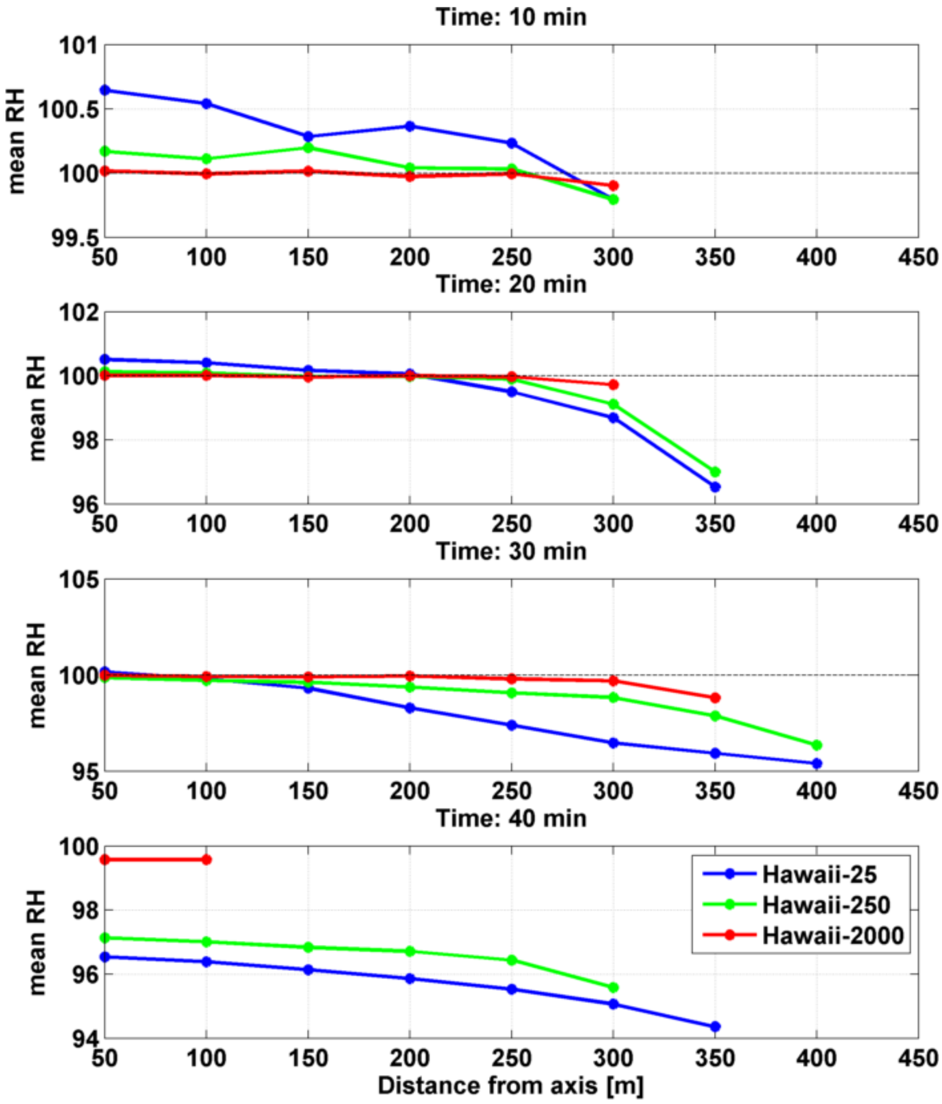
Time: 10 min
mean RH
101
100.5
100
99.5
50
100
150
200
250
300
350
400
450
Time: 20 min
mean RH
102
100
98
96
Time: 30 min
mean RH
105
100
95
Time: 40 min
mean RH
100
98
96
94
Hawaii-25
Hawaii-250
Hawaii-2000
Distance from axis [m]

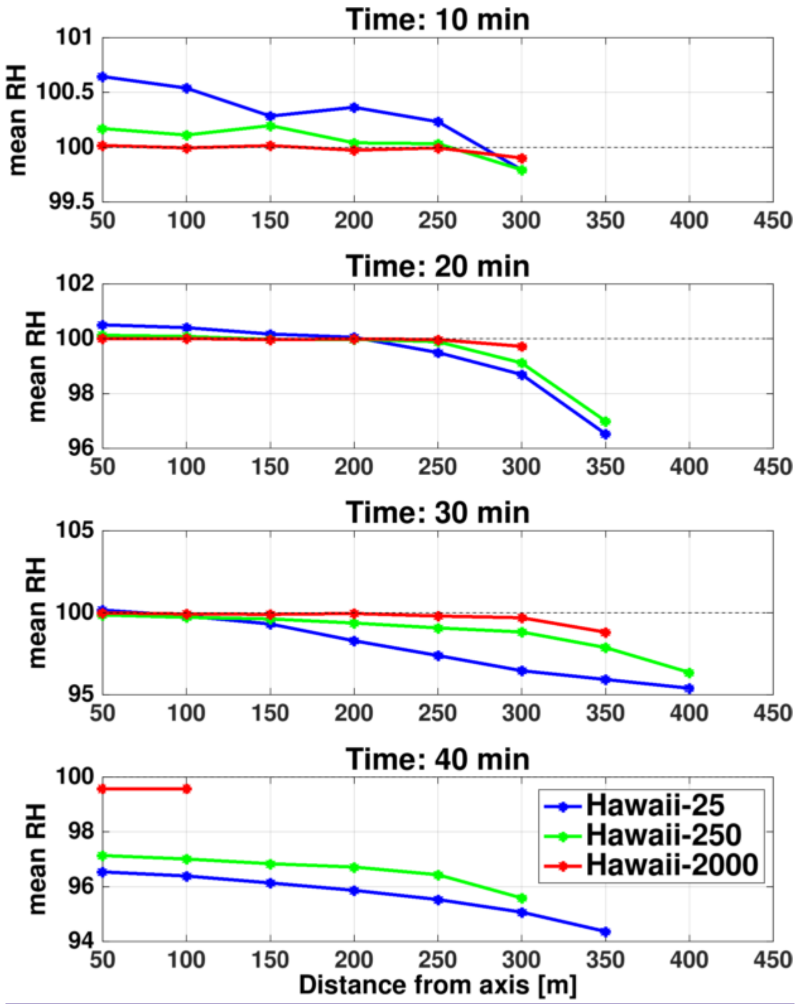

Figure 4. Four temporal snapshots (see panel titles for times) of RH [%] horizontal cross-sections. Panels include the results of different aerosol concentrations (see legend). Cross-sections are obtained by taking the mean RH of all vertical levels for each horizontal distance from the cloud center axis.

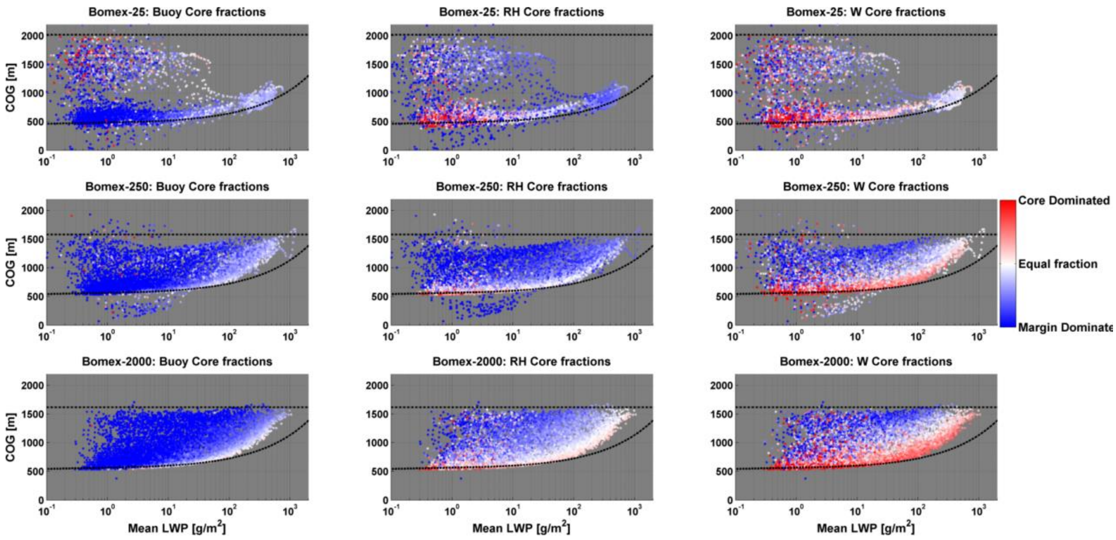
Bomex-25: Buoy Core fractions
Bomex-25: RH Core fractions
Bomex-25: W Core fractions
Bomex-250: Buoy Core fractions
Bomex-250: RH Core fractions
Bomex-250: W Core fractions
Bomex-2000: Buoy Core fractions
Bomex-2000: RH Core fractions
Bomex-2000: W Core fractions
COG [m]
Mean LWP [g/m^2]
Core Dominated
Equal fraction
Margin Dominate

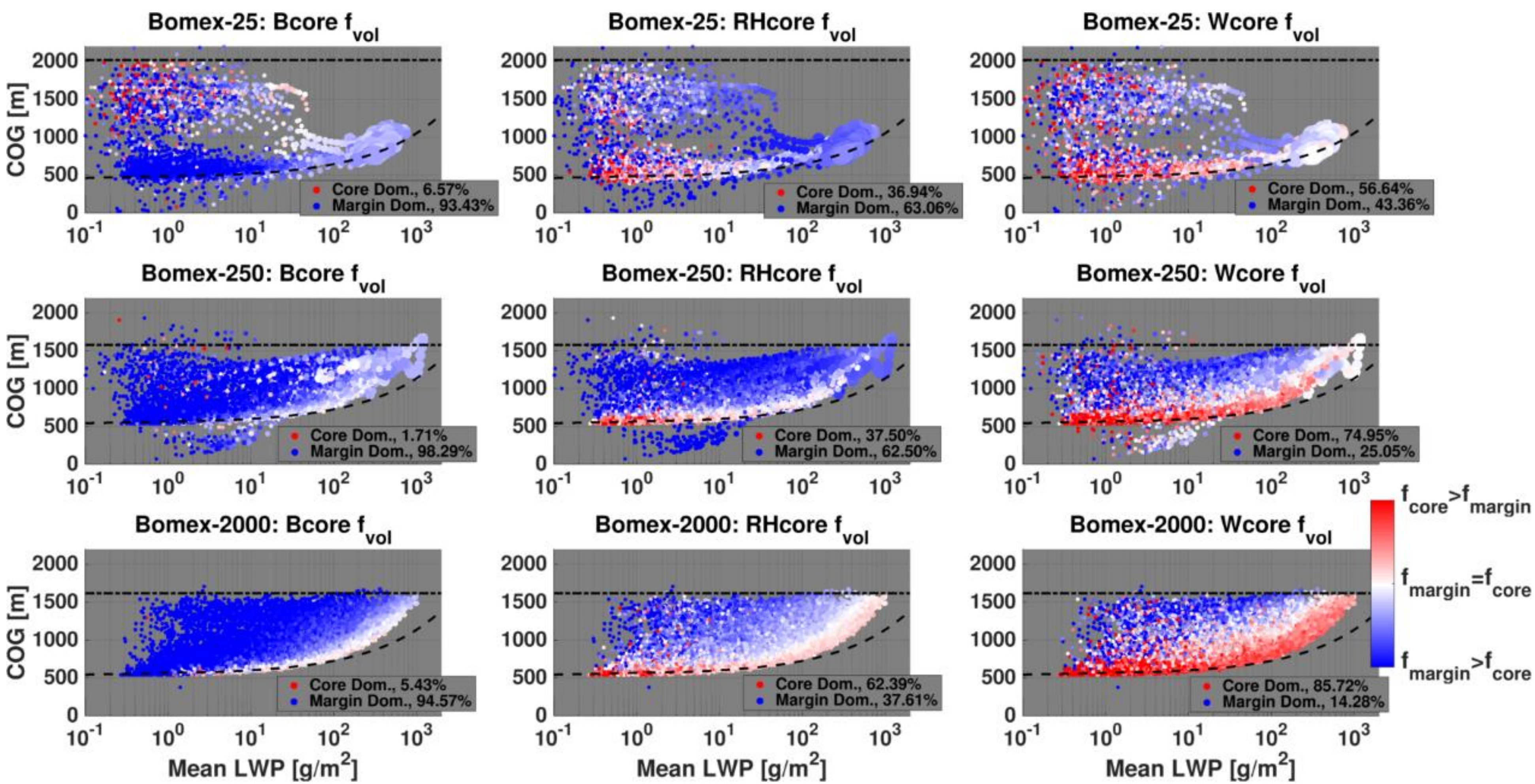

Figure 5. CvM phase space diagrams of Bcore (left column), RHcore (middle column), and Wcore (right column) volume fractions (f_{vol}) for all clouds between 3 h and 8 h in the BOMEX simulations. The upper, middle, and lower rows correspond to the clean, intermediate, and polluted aerosol cases. -The red (blue) colors indicate a core ~~volume fraction~~f_{vol} above (below) 0.5. The ~~majority of clouds are confined~~size of each point in the scatter is proportional to the ~~region between the adiabatic~~ cloud ~~growth approximation (curved dashed line) and~~mean area, where the ~~inversion layer base height (horizontal dashed line).~~smallest (largest) point corresponds to an area of 0.01 (11.4) km^2. The percentage of clouds

that are core dominated ($f_{vol} > 0.5$) is included in panel legends. For an in-depth description of CvM space characteristics, the reader is referred to Sect. 2.4 in PTI.

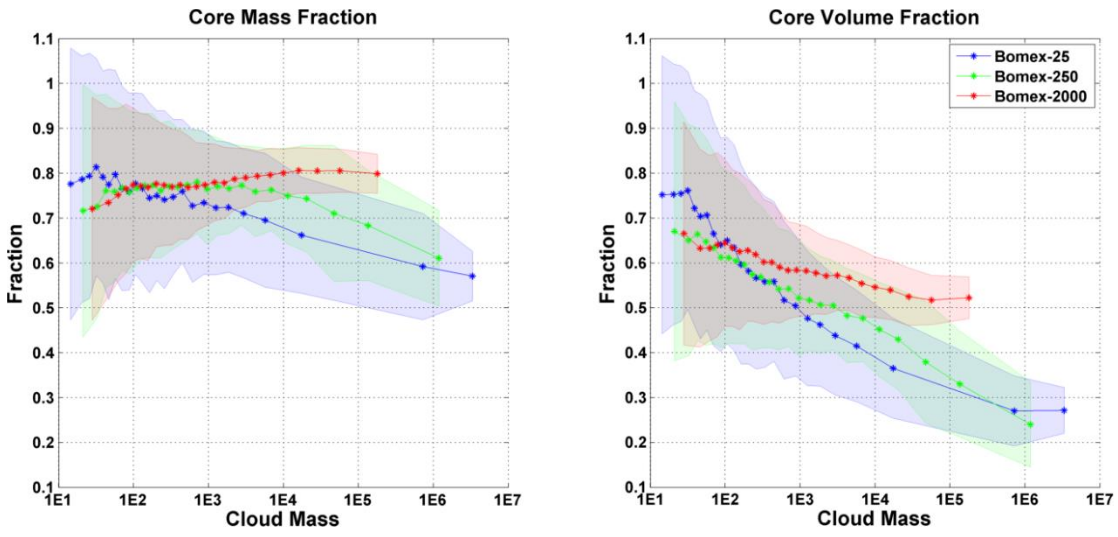

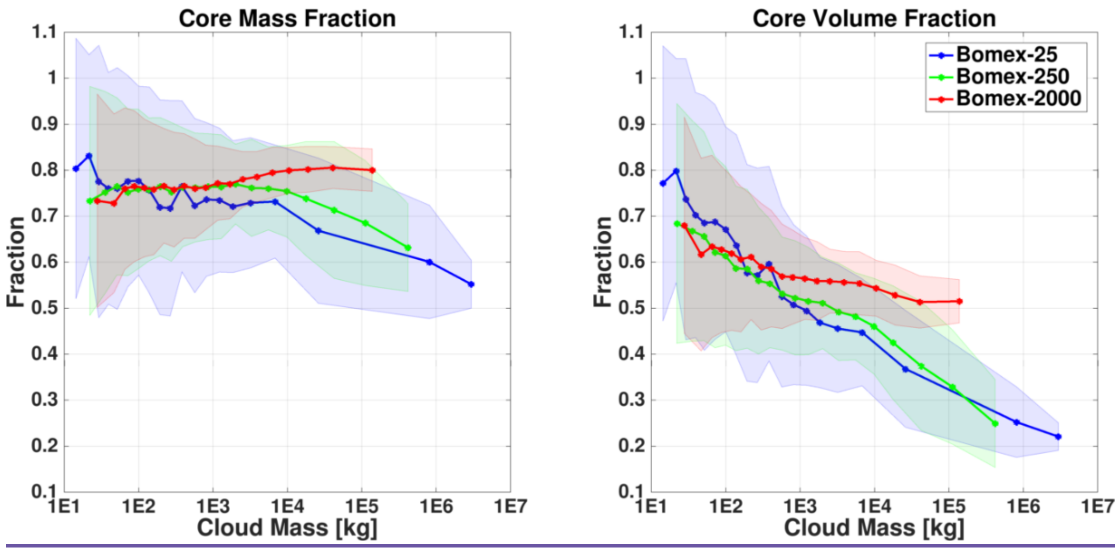

Figure 6. Average core mass fraction (left) and volume fraction (right) values for different aerosol concentrations, as indicated in the legend. The average only includes growing branch clouds from within the CvM space (i.e. clouds located in proximity to the adiabat). The core here is defined according to RH>100% definition.

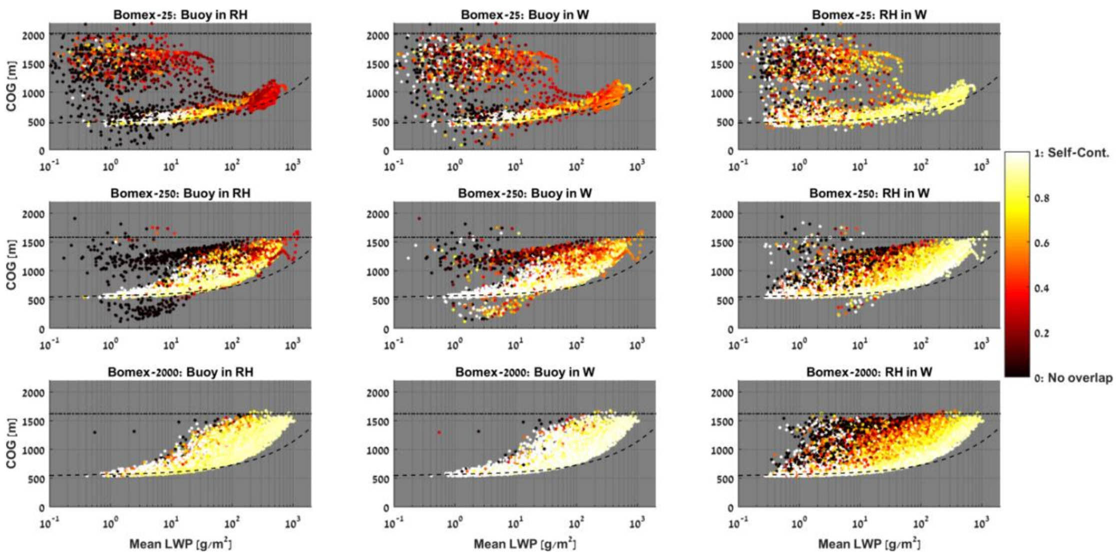

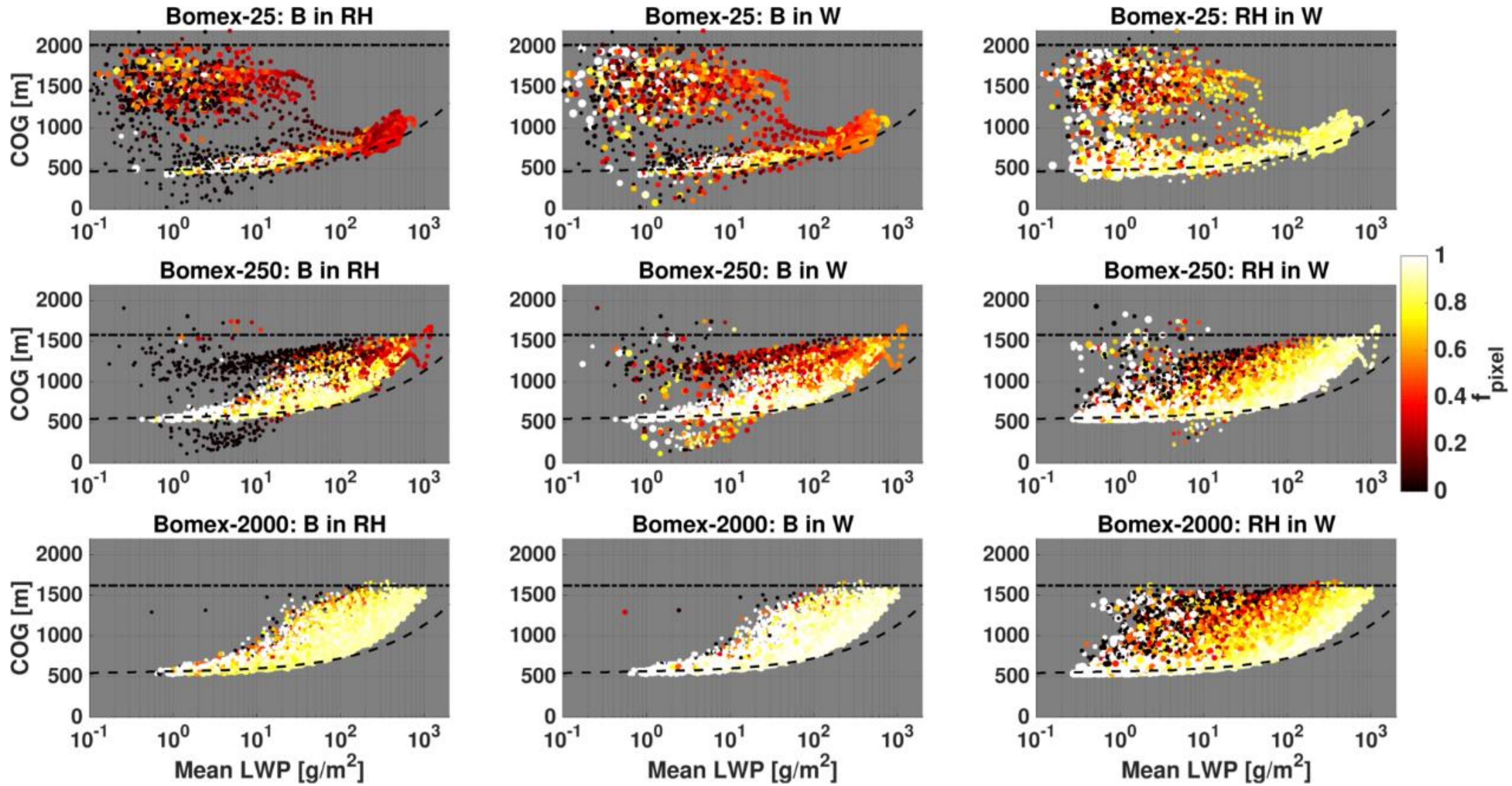

Figure 7. CvM space diagrams showing the pixel fractions (f_{pixel}) of Bcore within RHcore (left column), Bcore within Wcore (middle column), and RHcore within Wcore (right column), for the clean (top row), intermediate (middle row), and polluted (bottom row) simulations. Bright colors indicate high pixel fractions (large overlap between two core types) while dark colors indicate low pixel fraction (little overlap between two core types). The differences in the scatter density and location for different panels are due to the fact that only clouds which contain a core fraction above zero (for the core in question) are considered.

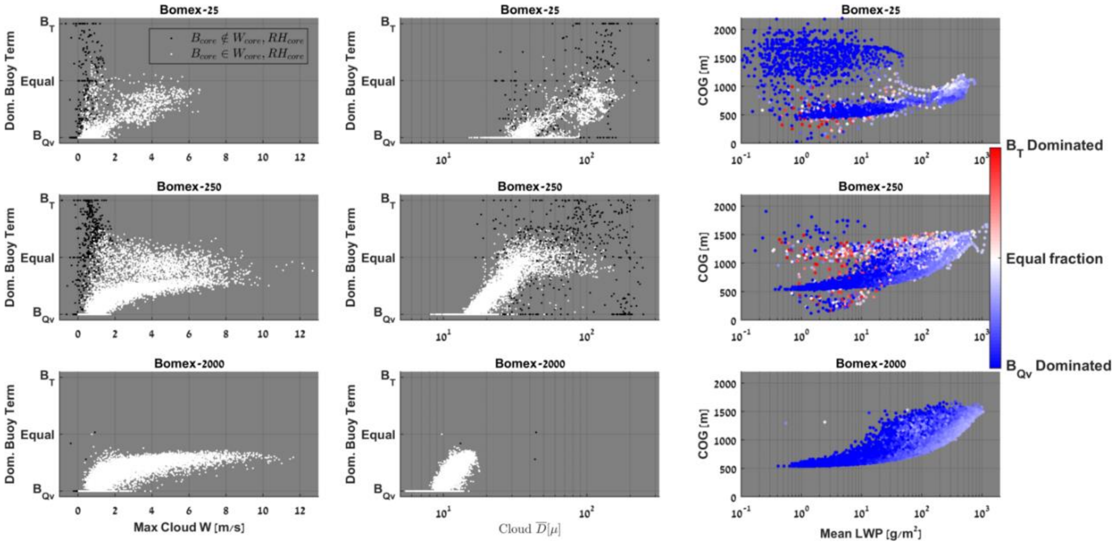
Bomex-25
Bomex-250
Bomex-2000
Dom. Buoy Term
B_T
Equal
B_{Qv}
$B_{core} \notin W_{core}, RH_{core}$
$B_{core} \in W_{core}, RH_{core}$
Max Cloud W [m/s]
Cloud $\overline{D}[\mu]$
COG [m]
Mean LWP [g/m^2]
B_T Dominated
Equal fraction
B_{Qv} Dominated

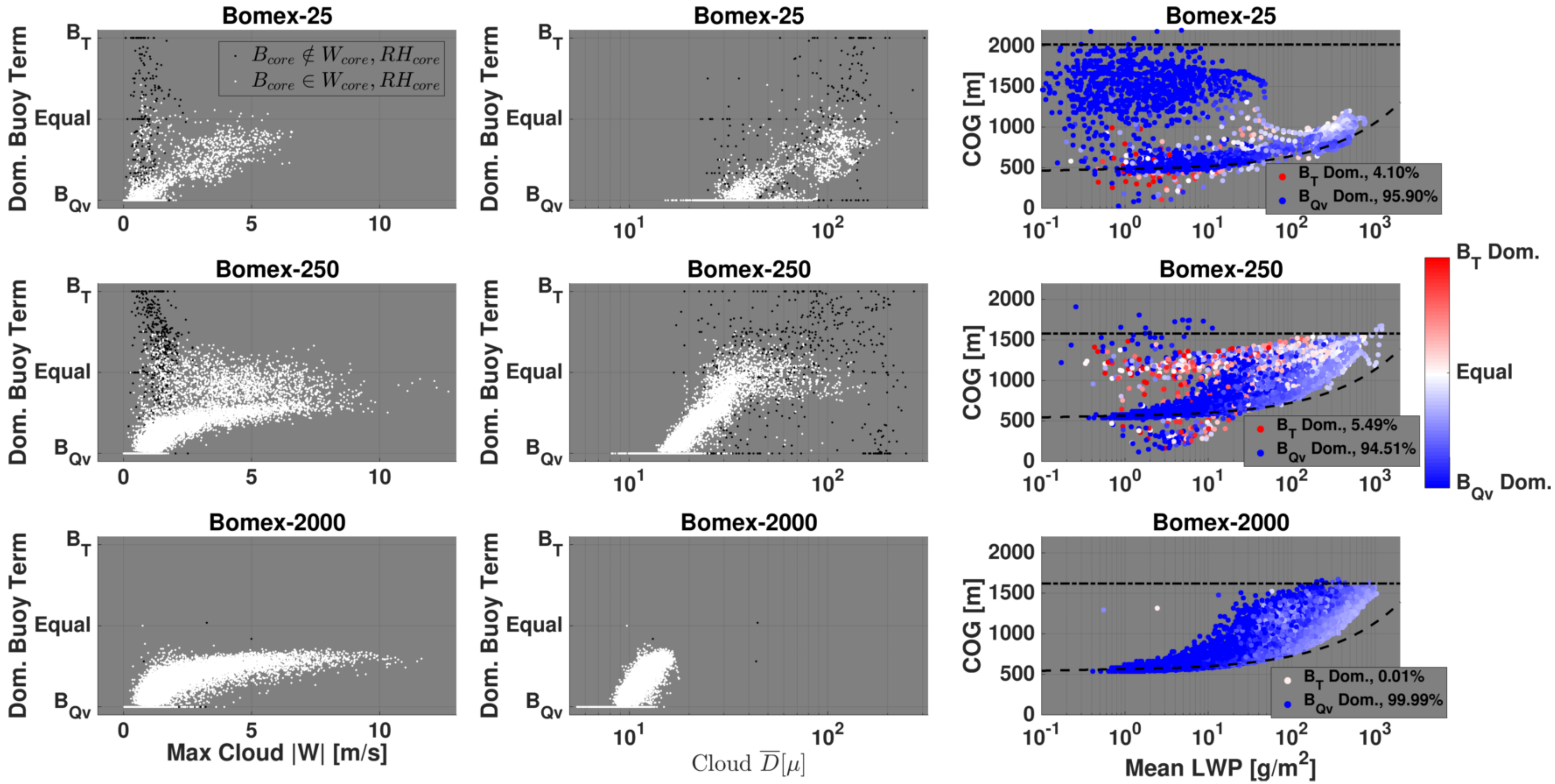

Figure 8. Analysis of dominant buoyancy term within ~~B_{core}~~Bcore of clouds (see text for details). As seen in previous figures, rows represent clean (top), intermediate (middle), and polluted (bottom) simulations. Left column: dependence on maximum absolute vertical velocity within cloud. Middle column: dependence on partition of total cloud mass to cloud droplets and rain drops. Right column: CvM space diagrams of all clouds with ~~B_{core},~~Bcore, where red (blue) shades indicate temperature (humidity) buoyancy terms dominate the cloud. Legends include percentage of clouds that are B_T or B_{Qv} dominated (see text for explanation).

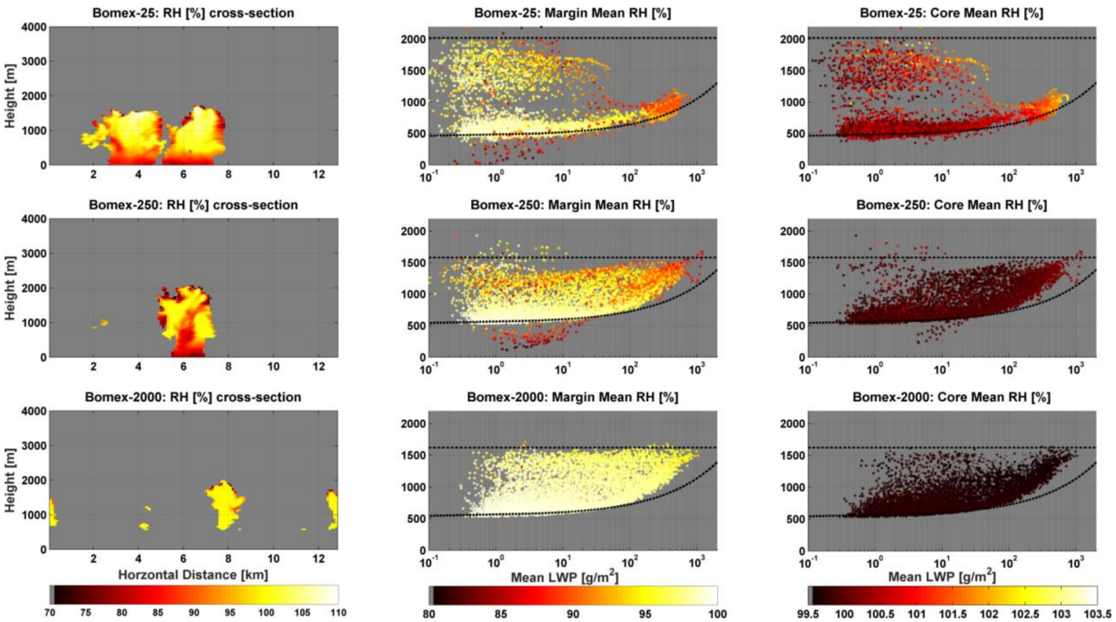
Bomex-25: RH [%] cross-section
Bomex-25: Margin Mean RH [%]
Bomex-25: Core Mean RH [%]
Bomex-250: RH [%] cross-section
Bomex-250: Margin Mean RH [%]
Bomex-250: Core Mean RH [%]
Bomex-2000: RH [%] cross-section
Bomex-2000: Margin Mean RH [%]
Bomex-2000: Core Mean RH [%]
Height [m]
Horzontal Distance [km]
Mean LWP [g/m^2]
70 75 80 85 90 95 100 105 110
80 85 90 95 100
99.5 100 100.5 101 101.5 102 102.5 103 103.5

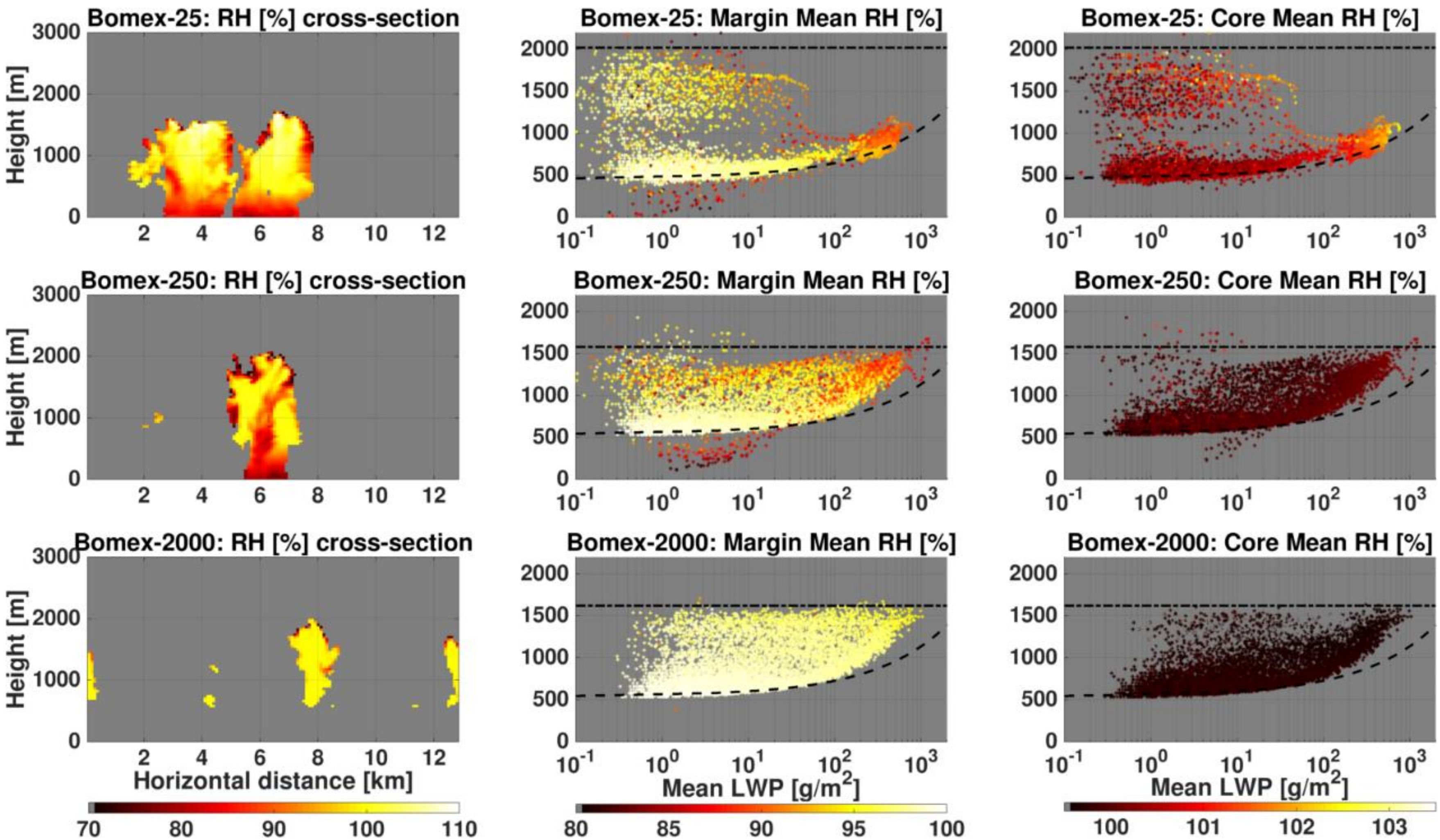

Figure 9. Left column – Relative Humidity (RH [%]) vertical cross-sections slicing through the center of gravity of the most massive cloud in each simulation. Middle and right columns display CvM space diagrams of mean cloud margin RH and mean cloud core RH, respectively, using the ~~RH_{core}~~RHcore definition. The upper, middle, and lower panels correspond to the clean, intermediate, and polluted aerosol cases (see panel titles). Notice the different color bar ranges for margin and core mean RH panels.